Study of Seismic Reflection Data over Virginia Mesozoic Basins

by

Gregory Thomas Schorr

Thesis submitted to the Faculty of the

Virginia Polytechnic Institute and State University

in partial fulfillment of the requirements for the degree of

Master of Science

in

Geophysics

APPROVED:

Cahit Çoruh, Chairman

John K. Costain

Lynn L. Glover III

September 25, 1986

Blacksburg, Virginia

Study of Seismic Reflection Data over Virginia Mesozoic Basins

by

Gregory Thomas Schorr

Cahit Çoruh, Chairman

Geophysics

(ABSTRACT)

Studies of Vibroseis reflection profiles over the exposed Triassic-Jurassic Culpeper, Richmond, and Scottsville Basins, and another profile over a probable early Mesozoic basin (Toano) beneath the Atlantic Coastal Plain sediments, in Virginia indicate that resolution of the geometry of the basins is inhibited by small impedance contrasts between the rock units within the basin and those bordering the basin. None of the seismic sections exhibit reflections which can be directly attributed to a Triassic-pre-Triassic interface. Resolution of the geometry of the basin sediments depends upon the presence of anomalously high or low velocity/density rock units within the basin, and similarly the presence of large amplitude reflections from within these and possibly other basins may imply the presence of these units, which include basalt and lignite. A method of analyzing the refracted waves in the seismic reflection data with large receiver offsets for determination of apparent velocities and the geometry of the refraction interface is presented. The Culpeper seismic lines indicate a basin with a maximum thickness of 2500 m along the western side and approximately 1750 m along the eastern side of the basin. The maximum thickness of the Richmond Basin below the seismic line is approximately 2700 m. The Scottsville Basin contains sedimentary strata with a thickness of 1750 m and the seismic data from the Toano Basin indicate a thickness of 3000 m. The compressional wave velocity of the strata within these basins has a range of 4000-5300 m/sec.

Acknowledgements

Many people have assisted me throughout my stay at Virginia Tech. My major advisor Dr. Çoruh patiently guided me in processing the data and never let steps go by unquestioned. Drs. John Costain and Lynn Glover III proofread the manuscript and made valuable suggestions concerning the processing and interpretation of the data respectively. Thomas Pratt made the initial subject recomendation and also made invaluable suggestions concerning processing and interpretation of the data. Thanks go out to Chevron, the Department of Geological Sciences, and ARCO for the money supplied which made my attendance a Virginia Tech possible. Data collected from the Scottsville Basin were collected and initially processed under grant # EAR-8009549-2 by Glover and Costain between 10/1/80 and 5/31/85. Data collected from the Richmond Basin were collected and initially processed under grant # NRC-04-75-237 by Glover and Costain between 8/75 and 5/15/85. All the data collected from the Culpeper Basin were supported by the Virginia Division of Mineral Resources grant # 848121-1 by Costain, Çoruh, and Glover 1981-4/30/83. Mildred Memitt and Bob Montgomery are the forces that keep the VAX facilities operating, and make it possible for the students to learn the use of the facilities quickly and thoroughly. When everyone else had gone, my fellow graduate students, in particular Dave Taylor and Stephen Scott provided some very thought provoking discussions, some of which actually concerned my data. My wife, Lisa, makes all of lifes trying times bearable and all of lifes enjoyable times truly special. Finally,

I would like to dedicate this paper to my mother and father who have taught me the value of hard work and dedication.

Table of Contents

List of Illustrations

List of Tables

Introduction

The exposed Mesozoic basins of Virginia are elongate structures (Figure 1) which tend to follow the general strike of the pre-Triassic Piedmont rock units. Similar basins are present beneath the Atlantic Coastal Plain on the basis of seismic reflection, drill-hole, and potential field data (Brown and others, 1972; Johnson, 1975; Petersen and others, 1984). The basins formed in Late Triassic and Early Jurassic times, and are related to the opening of the present day Atlantic Ocean (Cornet, 1977; Bally, 1981; Manspeizer, 1981).

As a part of several ongoing studies at the Regional Geophysics Laboratory (RGL), Department of Geological Sciences, at Virginia Tech, Vibroseis reflection data were obtained over the Culpeper, Scottsville, and Richmond Mesozoic sedimentary basins (Figure 1). Another Vibroseis reflection survey traversing most of the Piedmont and the Atlantic Coastal Plain in central and eastern Virginia was acquired for the U. S. Geological Survey by Geophysical Service Incorporated (GSI). Approximately 27 Km of this line over the Atlantic Coastal Plain has been included here after earlier reprocessing indicated the presence of a probable Early Mesozoic basin beneath the Coastal Plain sediments (Pratt, in preparation) which will be referred to herein as the Toano Basin because of its proximity to the town of Toano. All of the data were reprocessed at the RGL on a VAX 11/780 computer using Digicon's DISCO seismic software.

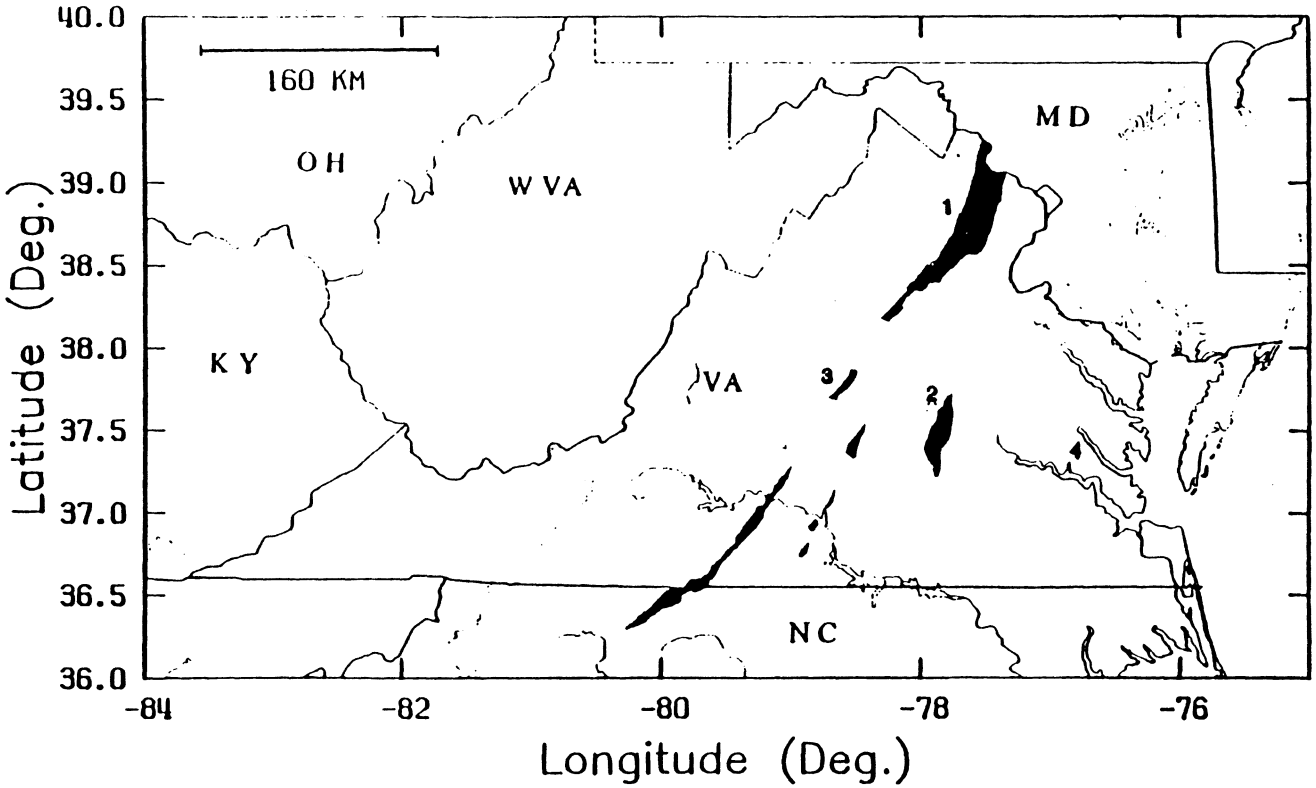

Figure 1. Index map of study area: Shows location of Culpeper (1), Richmond (2), and Scottsville (3) Basins and the general location of unexposed Toano (4) Basin.

The primary purpose of this study is to investigate and discuss similarities and differences in the subsurface geometries of the Early Mesozoic basins of Virginia based on the seismic data. This study also examines the effect of the various recording parameters used to acquire the data on the resolution obtained. Many of the seismic profiles obtained are poor quality data from the area of the basins, and the question of whether this is due to the way the data were recorded or the nature of the basins themselves (complex structure and or small velocity/density contrasts) is examined, with the aid of forward modeling. A method of employing the refracted arrivals in the seismic data for exploring the geometry of the basins is tested to see if it is a useful method for similar studies. In reviewing the acquisition and the processing of the data, suggestions are made concerning future seismic reflection studies of these and similar Early Mesozoic basins.

General geology

The general structure of the basins has been described as wedge-shaped half-grabens (Roberts, 1928; Bally, 1981; Manspeizer, 1981). The border faults of basins throughout the east coast may dip east or west, and are believed to be primarily listric normal faults (Bally, 1981). The border faults of the exposed basins of Virginia discussed in this study are located on the western edge of the basins and dip in an easterly direction (Roberts, 1928). Rock units within the basins tend to dip toward the border fault and may contain folds and secondary faults (Nelson, 1962; Lee, 1979 and 1980; Goodwin, 1970; Lindholm, 1979).

Basin fill is primarily continental red beds and carboniferous deposits, from fluvial, lucustrine, and paludal origins, and igneous intrusives and basalt flows (Roberts, 1928; Nelson, 1962; Lee, 1979 and 1980; Goodwin, 1970; Lindholm, 1979). Similar deposits from drill-hole data have been used to infer the presence of Mesozoic basins below the Atlantic Coastal Plain sediments (Brown and others; 1972; Petersen and others, 1984). These rock units consist of conglomerates, sandstones, siltstones, and shales of which the constituents were derived from nearby surrounding country rock (Roberts, 1928; Lindholm, 1979). Some of the southern basins, such as the Richmond and the

Scottsville, contain coal deposits, but the Culpeper in particular does not (Roberts, 1928). The exposed basins contain igneous intrusives in the form of sills and dikes and the Culpeper basin contains numerous exposed basaltic lava flows (Roberts, 1928; Lee, 1979 and 1980).

There is general agreement that the locations of the border faults were determined in part by preexisting structures: Lindholm (1978b) suggested that the border fault of the Culpeper basin may dip east because the foliation of the metamorphic rocks to the west of the basin dip east. Bobyarchick and Glover (1979) showed that the border fault of the Richmond basin is a reactivated Paleozoic mylonite zone referred to as the Hylas Zone. Other basins along the east coast of North America exhibit similar relationships to preexisting structure (Ratcliffe, 1971; Faill, 1973; Glover and others, 1980; Petersen and others, 1984).

Seismic Reflection Data

Approximately 68 Km of Vibroseis seismic reflection data from the Early Mesozoic basins of Virginia were reprocessed in this study. These data incorporated recording parameters ranging from 12-fold, long near-offsets (350 m) and receiver intervals (70 m) to 24-fold, short near-offsets (105 m) and receiver intervals (35 m), and all of the data were acquired using 48-channel field data acquisition systems. Some of the data resolved the subsurface geometry of the basins better than others. The seismic data are discussed in detail, including a general interpretation of the data and comparisons of the resolving ability of the various spread and recording parameters.

In the study of the data sets, special processing techniques were incorporated to help in the final interpretation. In particular, first breaks (refractions) from the available seismic data were studied in detail to determine velocities. Reduced refraction arrival times from the Richmond and the Toano Basins were analyzed to help image the subsurface geometry because of the longer spread configurations used to record those data. Discussions of some of the more important aspects of the processing are presented within each individual section.

The general processing of the data involved defining the geometry, correlation with Vibroseis whitening (VSW) (Çoruh and Costain, 1983), velocity and mute analysis, surface consistent residual statics, stacking, and migrating the data. A frequency-wave number (F-K) filter was applied to the data from the eastern Culpeper Basin to remove surface waves from the shot records. A more de-

tailed discussion of the processing of the data can be found in appendix A, and the results of the processing are discussed in detail for each data set in the sections which follow. Line drawings and interpretations have been derived from the migrated sections after comparisons with the unmigrated data. Velocities used to derive the depth of various events range from 4500 to 5000 meters per second and therefore may not be accurate for events deeper then 1.0-1.5 seconds.

Culpeper Basin

Two Vibroseis seismic reflection profiles were obtained in the Culpeper Basin (Figure 2). VDMR1 is located in the east central area of the basin and spans approximately 7.0 Km (Figure 2). VDMR2 is farther west and north of VDMR1 and has an approximate length of 10.0 Km (Figure 2). Both lines are perpendicular to the strike of the geology of the basin in general and are designed to help define the subsurface geometry of the basin despite a 10 Km gap present between the two lines along a dip line. In the following two sections, each line is discussed separately because of the differences in the quality of the data, which required different processing techniques.

Western Culpeper Basin

The western Culpeper seismic reflection profile (VDMR2) begins west of the surface exposure of the basin, over crystalline Paleozoic rocks (Chilhowee), crossing the western border fault, and traversing a series of moderately westward dipping basalt and sandstone units (Figure 2) (Espenshade and Clark, 1976; Lee, 1979; Leavy, Froelich, and Abram, 1983). The Catoctin Formation (greenstones) is exposed just to the east of the beginning of the seismic line and overlies the Fauquier Formation, which consists of metamorphosed sedimentary strata (Figure 2) (Espenshade and Clark, 1976).

Data from the Culpeper Basin are 24-fold and have a symmetrical split-spread shot configuration. The receiver interval and the near offset are 35 m and 105 m respectively, and the data were acquired with a downsweep of 58-10 Hz with a sweep length of 18 sec. The data were processed

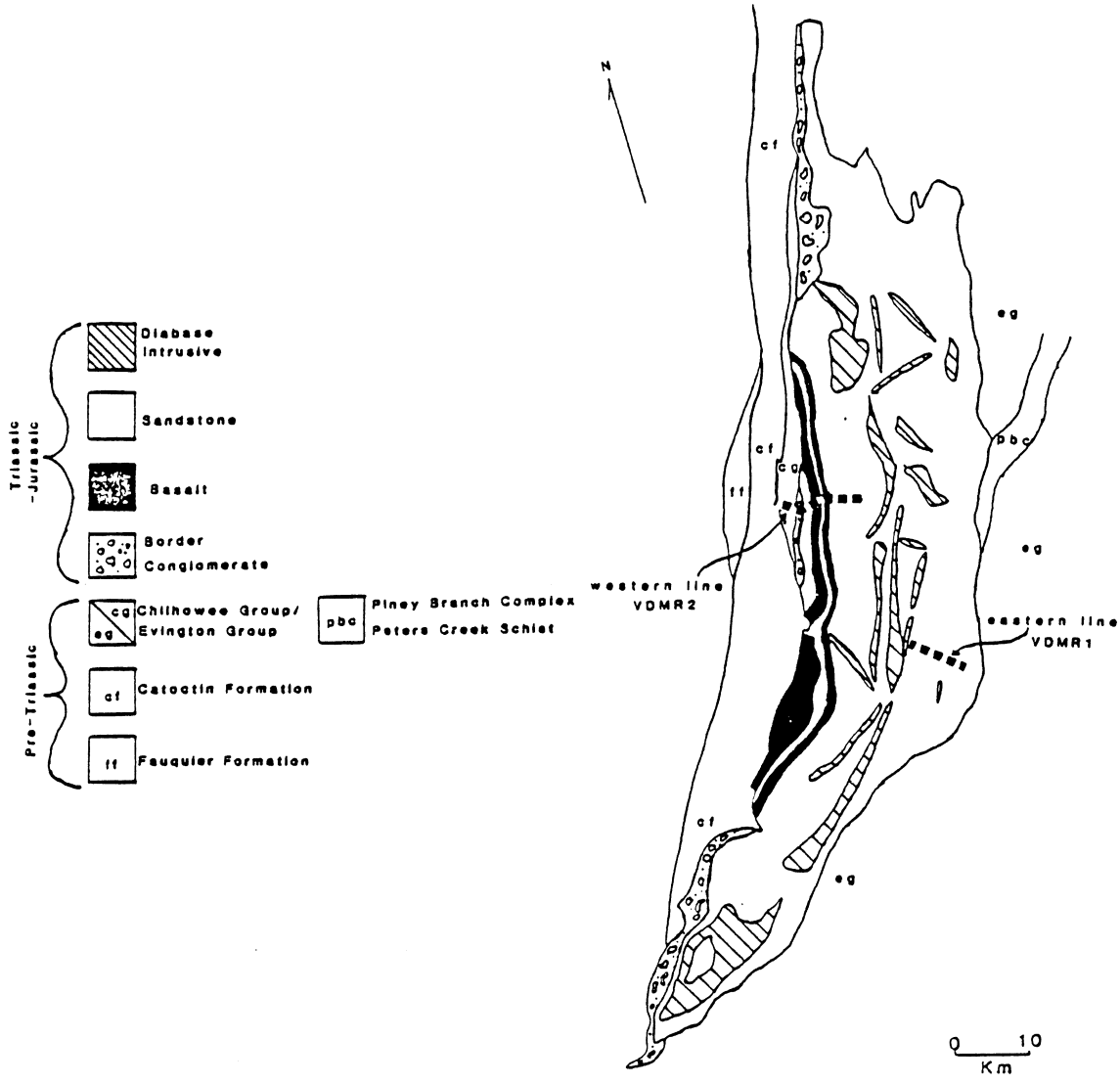

Figure 2. Geology of the Culpeper Basin: With location of the seismic lines (location 1 from Figure 1) (modified from Leavy and others, 1983; and Espenshade and Clark, 1976)

in a standard manner (see appendix A). In general, the quality of the data is good with large amplitude events clearly imaged. The only drawback to the data quality was a ringy appearance which was removed with the application of a predictive deconvolution filter using a gap of 20 msec and length of 80 msec. Special emphasis was placed on velocity and mute analysis because reflections from within the basin here have a maximum two-way travel-time of only 0.8-1.0 sec. Stacking velocities for this data had a range of 4500-7000 m/sec and there were no clear apparent velocity patterns present which might relay information concerning the nature of the basin. The high stacking velocities are attributed to the fact that the strata within the basin dips as much as 40° (Lee, 1979 and 1980). Because the velocities had such a large range in such a relatively short time span, defining a mute pattern was especially important to remove the effects of the stretching due to normal move out (NMO) corrections and still extract information from the upper 0.2 sec of two-way travel-time. Several methods of picking a mute pattern were attempted including examination of every fifth common-mid-point (CMP) gather after NMO corrections.

After deriving a stacked section, the data were migrated using a finite-difference time migration routine. Figure 3 shows a stacked two-way travel-time section before migration, and contains numerous reflections with a high signal-to-noise ratio (S/N). After migration (Figure 4) events are relocated, and the S/N increased and many subhorizontal reflections at 0.5-1.7 sec have increased continuity despite the poor velocity control (Figure 4). Before migration, the area below stations 55-70 was free of reflections (Figure 3) which suggests a vertical discontinuity, but after migration, events from 1.0-2.0 sec have been moved up and into much of the area by the migration process thereby increasing the continuity and the S/N of the data in that area. This implies that the apparent break in the data is not vertical through the entire section in time.

The reflection data can be divided into three distinct groupings (Figure 4). Between stations 80-280 at the top of the section are a group of large amplitude reflections which have apparent westward dips of 25°-45° ("A" in Figure 4). These are most concentrated below stations 120-200 at 0.0-0.4 sec (Figure 4). Other similar reflections can be seen below station 270 at 0.2 sec, below station 240 at 0.6 sec, and below station 90 at 0.2 sec (Figure 4). Below these westward-dipping reflections are a group of reflections which are subhorizontal in the central portion of the section

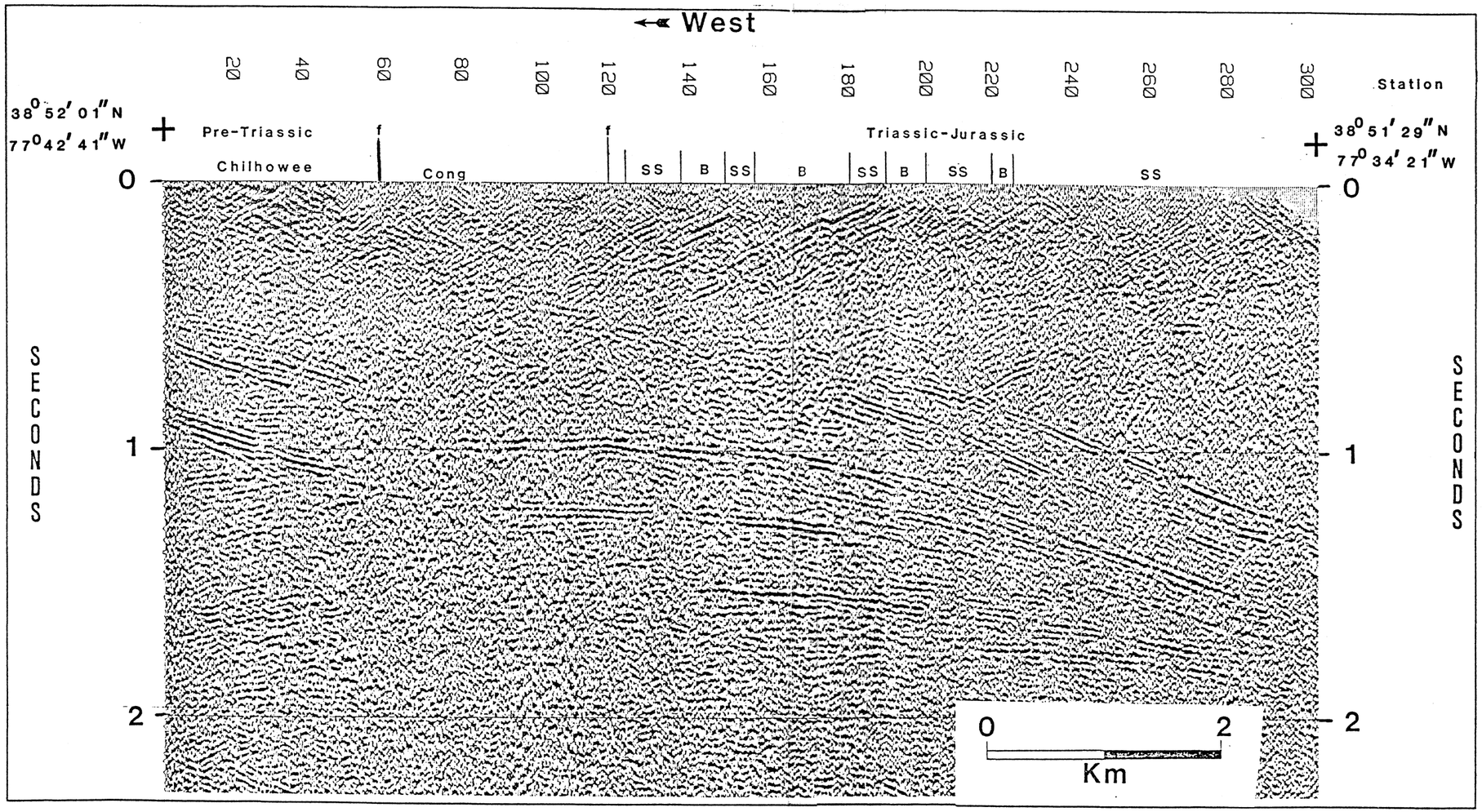

Figure 3. Western Culpeper Basin: Stacked section prior to migration; surface geology from Lee (1979) and Espenshade and Clark (1976). Cong-conglomerate, SS-sandstone, B-basalt, f-fault.

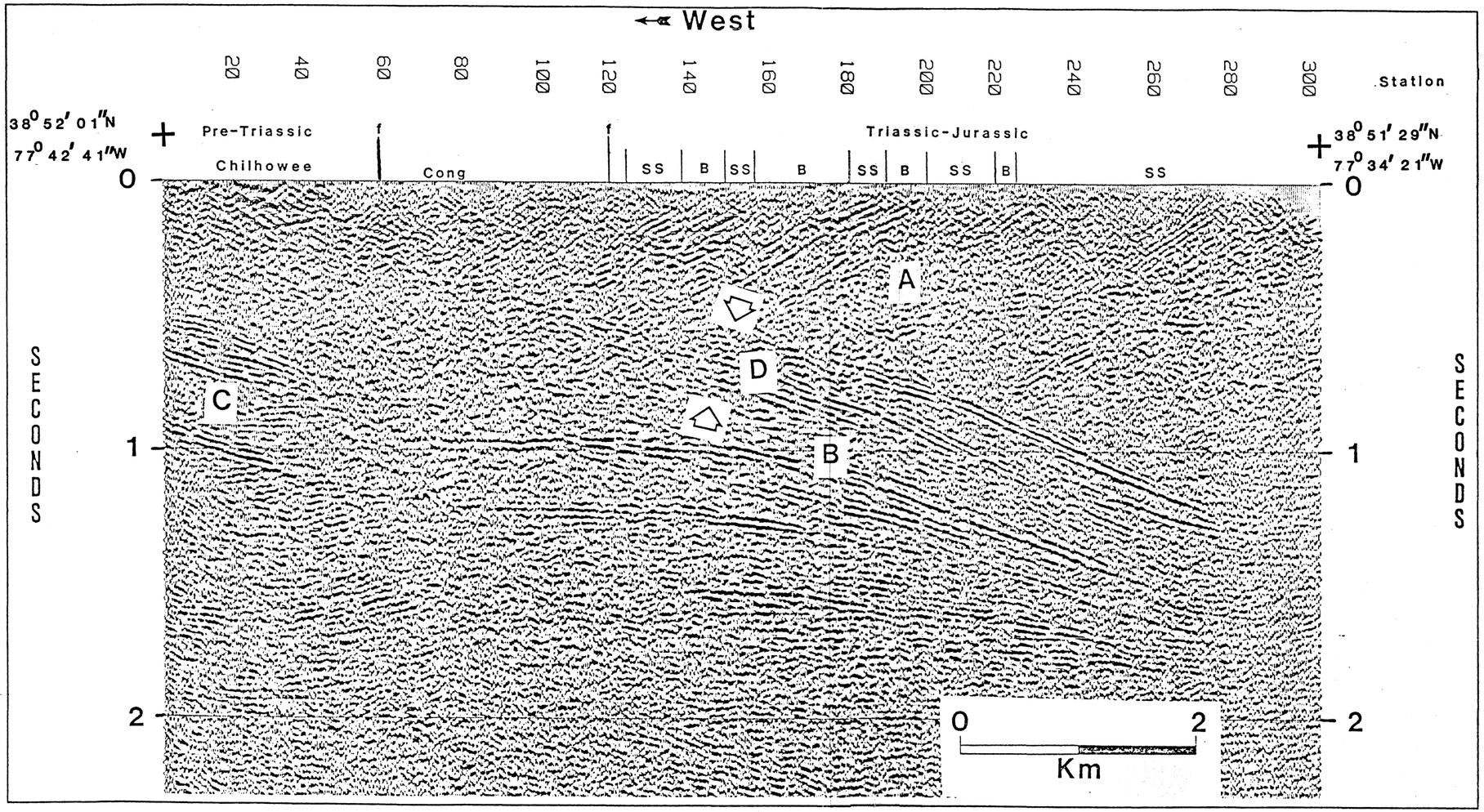

Figure 4. Western Culpeper Basin: Time migrated section; surface geology from Lee (1979) and Espenshade and Clark (1976). Cong-conglomerate, SS-sandstone, B-basalt, f-fault.

and acquire an apparent eastward dip of as much as 25° as they are traced from station 100 at 0.4-1.5 sec to below station 250 at 1.0-1.8 seconds ("B" in Figure 4). These reflections are the most continuous below stations 200-280. West of station 150, below the high concentration of westward-dipping reflections, much of this continuity is degraded down to 0.9 sec, even after migration ("D" in Figure 4). The third group of reflections occur below stations 0-55 at 0.5-1.1 seconds ("C" in Figure 4). These are numerous, concentrated, and have an apparent eastward dip of 25°-35°.

These data have been modeled using AIMS (Advanced Interpretive Modeling System, a product of Geoquest International, Incorporated) software package. This is the only section that has been modeled because of the high S/N, good resolution, and the ability to correlate much of the surface geology with the reflections. The first group of westward-dipping reflections ("A" in Figure 4) have been modeled as layered basalt and sandstone units, which have been faulted in two places. This was derived from the correlation of these reflections with the mapped surface geology of Lee (1979). Below stations 100-200 an eastward-dipping diabase intrusive has been included in the model. This correlates with reflections seen in the same general area of the migrated section (Figure 4). Another diabase intrusive has been included at 0.5 seconds below stations 190-300 from the migrated section. These diabase intrusives have been included because of their prevalence at the surface (Lee, 1979 and 1980). The border fault of the basin has been brought in at station 60, based on correlation with the surface geology (Lee, 1979), with a general eastward dip of approximately 50°, based on measurements by Lindholm (1978b). Basin fill just east of the border fault has been modeled as low velocity/density conglomerate. The border fault in the model becomes listric and can be followed either to above or below a high-velocity layer of rock interpreted to be crystalline pre-Triassic rock ("D" in Figure 4). Two similar rock units have been added below this event. These two units are tied to a near-vertical fault interface below stations 50-60. The main reason for this tie is due to a limitation of the AIMS package requiring all horizons to be tied or closed; the fault, however, is interpreted to exist in this general area because of the marked change in the character of the reflections on either side. The high-amplitude eastward-dipping reflections ("C" in Figure 4) have been modeled as layered high-velocity/density and low-velocity/density rock units. The final model with velocities and densities used is shown in Figure 5. The velocities and

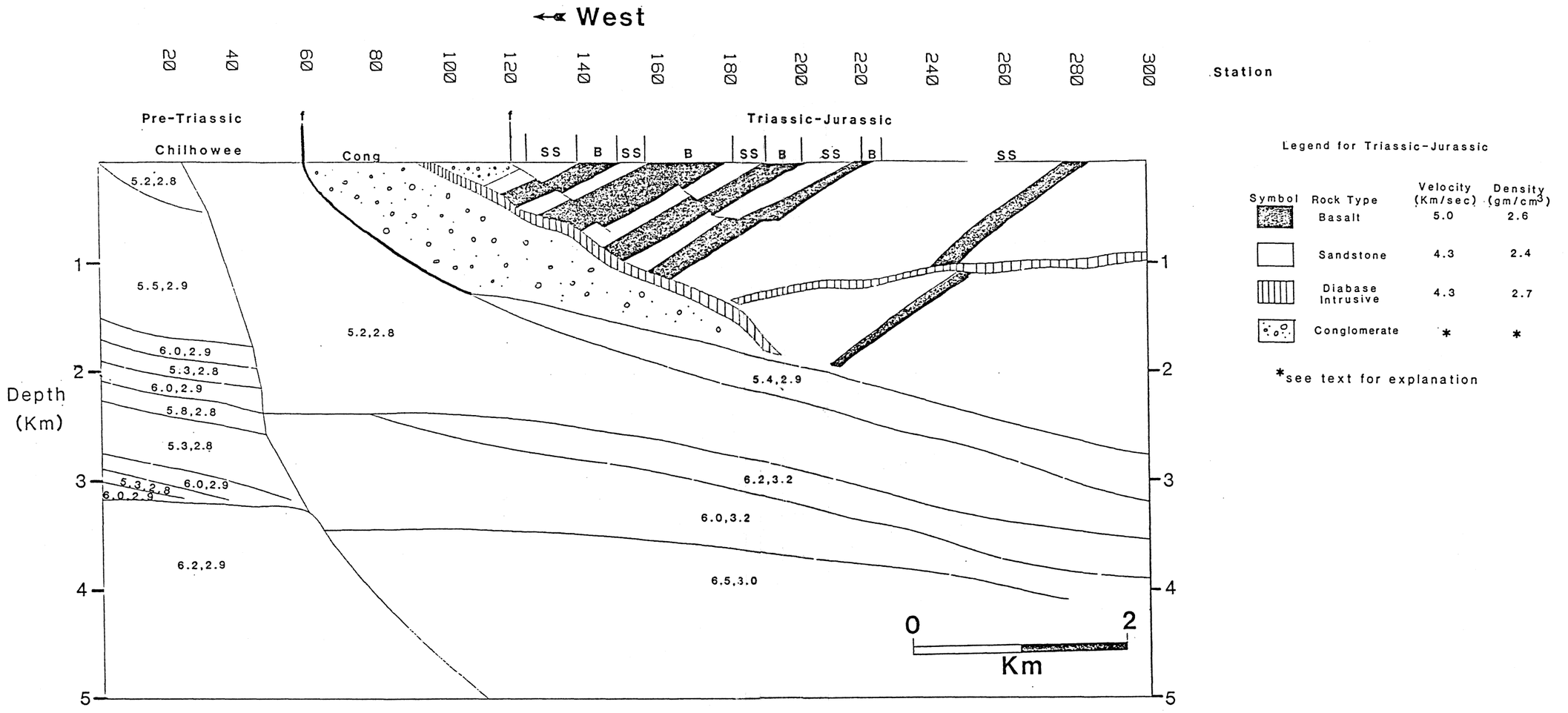

Figure 5. Depth model of the western Culpeper Basin: Model input to AIMS for ray tracing derived initially from a two-way travel-time model. Numbers 4.3,2.4 represent the interval velocity and density in Km/sec and gm/cm^3 respectively.

densities have been taken from Bonner and Schock (1981) and Brennen (1985). The velocity and density of the conglomerate rock unit within the basin varied with depth with the velocity at the surface being 3800 m/sec and reaching a maximum of 4000 m/sec and the density at the surface being 2.3 gm/cm^3 and reaching a maximum of 2.4 gm/cm^3.

Construction of the model began with a line drawing from the migrated section that was interpreted for a gross geometry. The model was derived in two-way travel-time and later converted to depth based on the interval velocities shown in Figure 5. The depth-converted model was smoothed to remove the more drastic effects of velocity pull-up and push-down which resulted during the time-to-depth conversion. All of the intersections of two or more different rock types were marked as diffractors. Normal incident zero offset ray tracing was carried out, and these rays were sorted into CMP order with an interval of 34.5 meters, which is double the actual CMP interval, in order to reduce the amount of computer time necessary to perform the ray tracing. Spike series were derived and convolved with a Klauder wavelet operator (inset Figure 6) of length 0.24 sec and frequency content of 10-58 Hz. An exponential gain was applied and white noise was added at a rate of 24 dB down from the highest amplitude event. A bandpass filter with Hamming-designed ramps of 8-12 Hz on the low end and 38-57 Hz on the high end was applied to the data.

The results of this modeling are shown in (Figure 6). The similarities between the model and the actual unmigrated section (Figure 3) lend plausibility to the interpretation which follows. The group of layered and faulted sandstone and basalt rock units provide a likely explanation for the near surface reflections seen in the actual data ("A" in Figure 4). The modeling implies that the faulting in the actual basalt/sandstone layers may be more extensive than that of the model. The resolution of the reflections from the diabase intrusives in the modeled section (Figure 6) also lend support to that interpretation. The border fault was not imaged despite a large reflection coefficient provided between the border conglomerate and the pre-Triassic rocks to the west ($0.20 < R < 0.25$). This also correlates with the actual data and can now be attributed the steep dip of the fault and the fact that rays traced through the complex of sandstone and basalt in many cases may not have been received. An important observation from the modeling is that reflections from immediately below the sandstone basalt series are not as continuous as reflections on either side of that area.

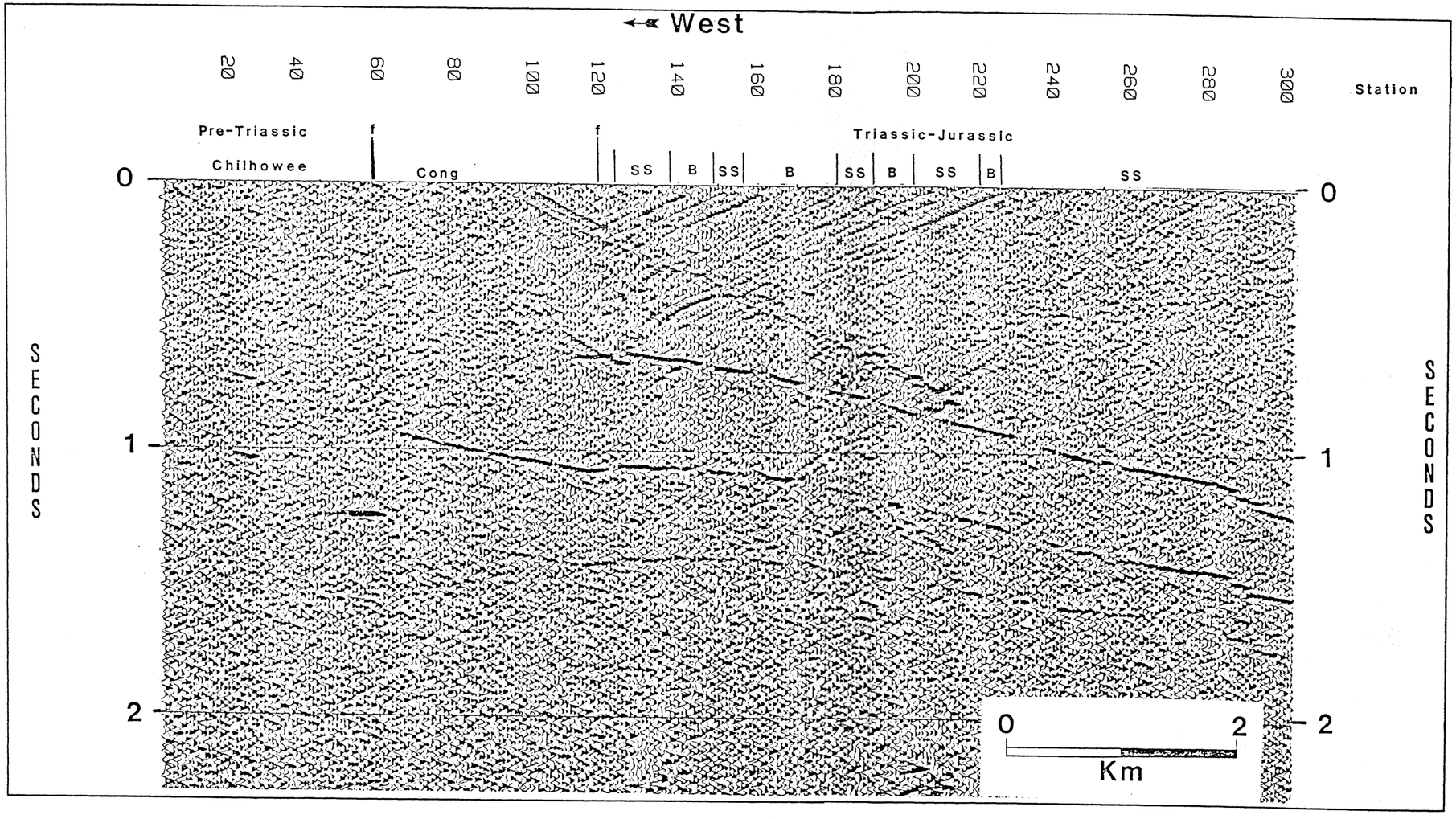

Figure 6. **Synthetic seismic section for the western Culpeper Basin:** Model of the unmigrated section in two-way travel-time; surface geology from Lee (1979) and Espenshade and Clark (1976). Cong-conglomerate SS-sandstone, B-basalt, f-fault.

This agrees with what is seen on the actual data and helped in the interpretation of data over similar basins. Another important observation from the modeled data is that despite well-defined diffractor points in the areas of the numerous discontinuities in the model, few of the diffractions are recognized. This correlates with the actual data and implies that because of the number of diffractors present, the events are canceling and/or obscuring one another. On the actual unmigrated section (Figure 3) diffractions are not recognized at all. This may be due to the fact that the actual data is more complex than the modeled section. Therefore, a lack of diffractors seen on seismic profiles can imply complex discontinuous structure rather than simple continuous structure depending on the noise level of the data. Reflections ("C" in Figure 4) from the area west of the basin were reduced to a short group of weak, reflections in the modeled section (Figure 6). This is partly attributed to the fact that the modeled beds are concave upward, which would narrow the area at the surface from which these rays would emerge. It is possible that the steep eastward dipping fault in the model (Figure 5) below stations 20-40 may have affected the ray tracing more than is observed in the actual data implying a smaller reflection coefficient at the fault interface for the actual data. Another reason for the small grouping can be attributed to the fact that the model did not continue beyond the far western edge of the actual migrated seismic section (Figure 4). Before migration (Figure 3) these events extend to below station 50 at 0.6-1.1 sec, but after migration much of the reflections have been pushed up and out of the western edge of the seismic section. Thus, part of these reflections came from west of the beginning of the migrated seismic section, indicating that they continue, for a short interval at least, unfaulted.

Figure 7 shows a line drawing and general interpretation derived from the migrated section and the modeled data. Studies of the refractions in the shot data indicate velocities near the surface of the basin of approximately 4500 m/sec, which were used to determine the depths of the events in the interpretation. The figures are at an approximate scale of 1:1 based on this velocity.

With the aid of the modeling, a general interpretation of the of the western Culpeper seismic profile is now possible. The basin is bordered by a listric fault which may related to an older structure (Figure 7). Whether the fault continues above the uppermost event marked "D" in Figure 4 or below below it is not resolved from the seismic data. Basalt-sandstone interfaces pro-

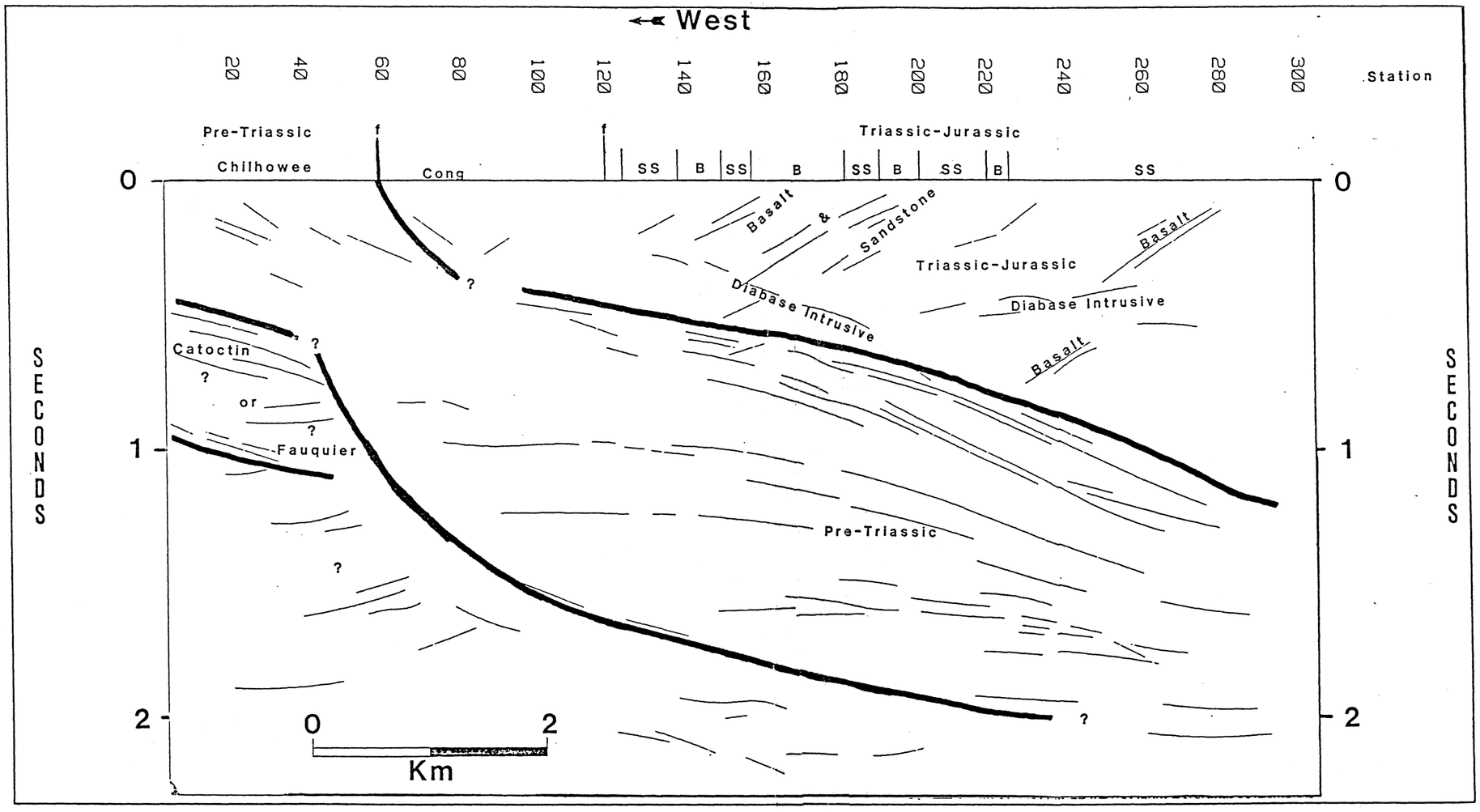

Figure 7. Western Culpeper Basin: Line drawing and interpretation; surface geology from Lee (1979) and Espenshade and Clark (1976). Cong-conglomerate, SS-sandstone, B-basalt, f-fault.

vide reflection coefficients ($0.08 < R < 0.11$) large enough to cause large amplitude reflections from within the basin where these rock units contain numerous faults. Diabase intrusives are one possible explanation for the weaker subhorizontal and eastward-dipping reflections seen within the basin because of the lower reflection coefficient derived from diabase/sandstone interfaces implied from the modeling, and the abundance of these intrusives seen at the surface (Lee, 1980). The interface between the Triassic-Jurassic rocks and the pre-Triassic rocks below them does not provide a large enough reflection coefficient ($R < 0.02$) to allow resolutions of reflections from this interface; the pre-Triassic rock units below must provide excellent velocity/density contrast to give such large and numerous reflections. An alternative explanation is that tuning (Sengbush and others, 1961) of the wavelet is occurring in thinly-bedded crystalline rocks. This hypothesis has been suggested and tested and found feasible for the Catoctin formation on the western side of the Blue Ridge Anticlinorium (Brennen, 1985).

An important observation from the actual migrated seismic section (Figure 4) is that the events which have been attributed to reflections from Triassic material never merge with, or are truncated by, an apparent reflection, which can be attributed to the interface between Triassic and pre-Triassic rocks. This is most evident on the westward dipping reflections below station 240 at 0.5-0.7 sec (Figure 4). This indicates that this interface does not provide a reflection coefficient large enough to resolve reflections from it. The high velocities derived from the refractions on the shot data (4500 m/sec) at the surface indicate that the velocities for Mesozoic sediments within these basins may be near to the velocities of the pre-Triassic rocks around them. Note that a detailed velocity analysis of the data is not possible due to the dipping interfaces and the complex geometry, which implies stacking velocities and velocities derived from velocity spectra (Tanner and Koehler, 1969) are not the true RMS velocities.

Eastern Culpeper Basin

The eastern Culpeper reflection profile (VDMR1) was conducted over the Balls Bluff Siltstone, which dips gently west 5°-10° (Figure 2) (Lee, 1979 and 1980). The line began just west of the

normally-faulted eastern border and is terminated just east of a mass of diabase dikes (Figure 2), which appear to split the basin along the long axis (Leavy and others, 1983; Lee, 1979 and 1980).

These data were acquired with the same recording parameters as the western Culpeper line. Processing of this data differed in two respects: (1) no predictive deconvolution filter was applied to the data because the data and autocorrelations of the data show no reverberations, and (2) a frequency-wave number (F-K) filter was applied to the shot data to remove the effects of a surface wave which dominated the first second of the shot records (see Appendix A). The F-K filter was applied in a rather unconventional manner: the shot data were split into negative and positive offset groups; a filter was applied to remove coherent events dipping 12-25 msec/trace for the positive offsets (1400-2750 m/sec), and one was applied to remove events dipping -25 to -12 msec/trace for the negative offsets. If the data were kept in their original shot order, then a filter would have to have been designed to remove all events in the range of -25 to 25 msec/trace. This is a much wider window in the F-K domain and would have resulted in poorer quality filtering (March and Bailey, 1982). Another alternative would have been to sort the shot data by absolute value of the offset and then filter with the smaller (12-25 msec/trace) window, but in resorting the shot data the coherency of the surface wave is degraded which again reduces the effectiveness of the filter.

An unmigrated section is shown in Figure 8. The same section after migration is shown in Figure 9, and Figure 10 shows a line drawing and interpretation which has been derived from the migrated section. One of the most notable reflections on the data ("A" in Figure 9) begins on the far eastern side of the section at 0.2-0.3 sec (470-705 m, based on a velocity of 4700 m/sec). This event has an apparent westward dip of 5° and steps down to the far western side of the section at 0.6-0.7 sec (1440-1690 m based on a velocity of 4800 m/sec. One interpretation of this event is that it originated from a highly reflective rock unit, or a series of them, from within the basin (basalt or basalt-sandstone interlayered). This would explain the multilobe nature of the reflected wavelet. This also agrees with the apparent lack of reflectivity from the Triassic pre-Triassic interface derived from the western Culpeper seismic section. An interpretation of the reflection as originating from the bottom of the basin fails to explain either of these facts. The breaks in this reflection below station 40 and below station 145 are interpreted to be due to faults at the bottom of the basin. The

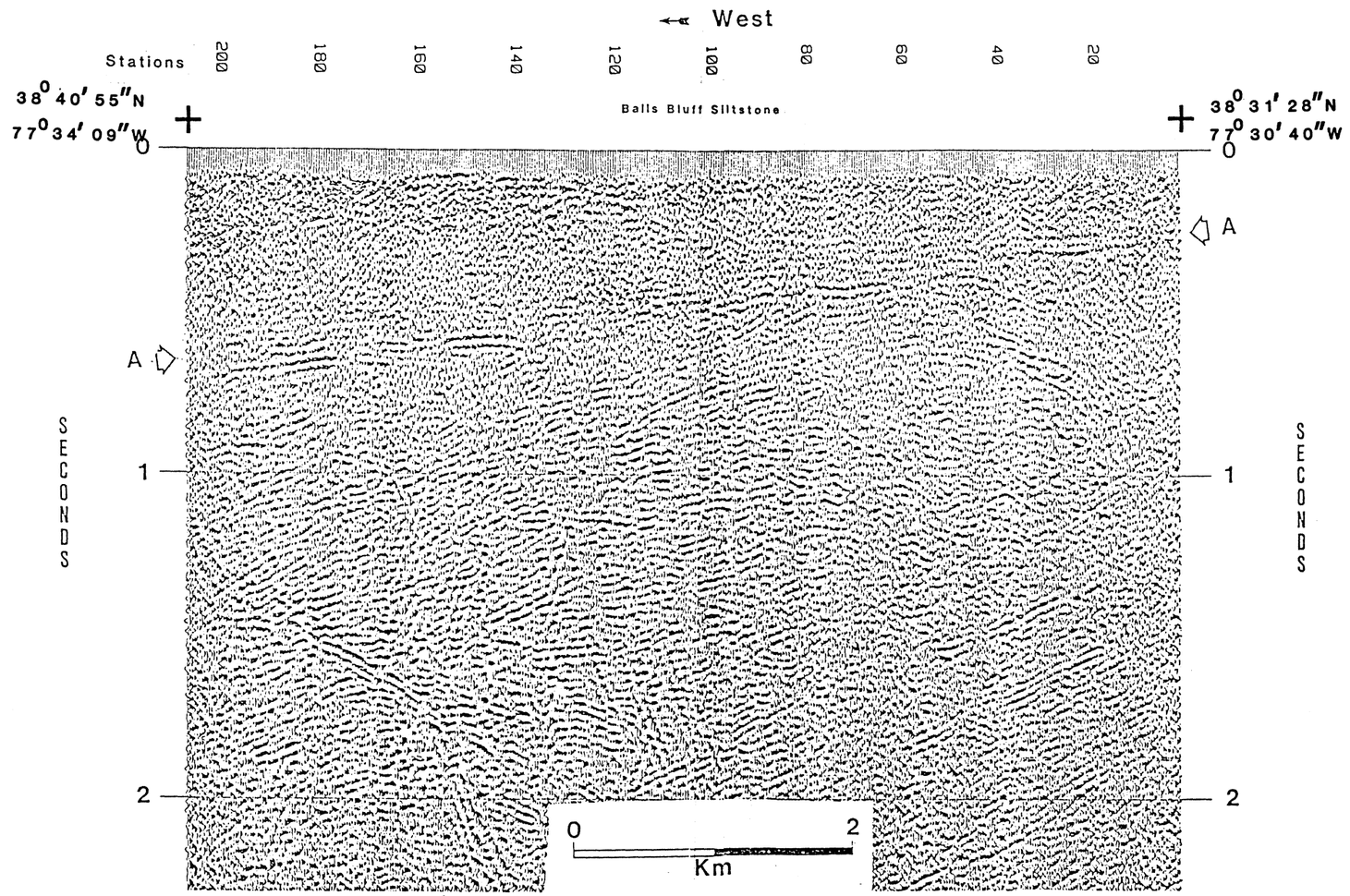

Figure 8. Eastern Culpeper Basin: Unmigrated seismic section with surface geology from Lee (1979).

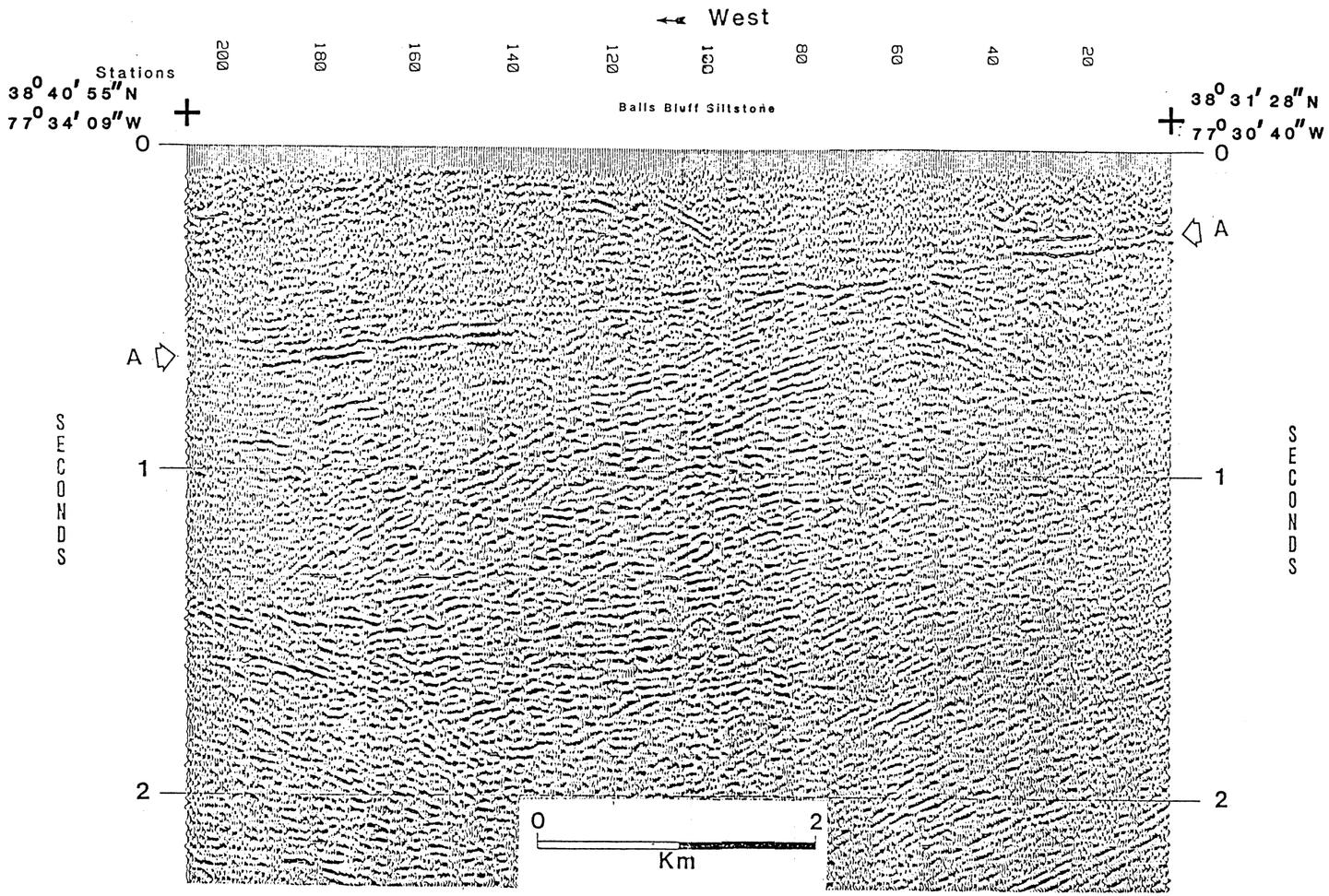

Figure 9. Eastern Culpeper Basin: Time migrated section with surface geology from Lee (1979).

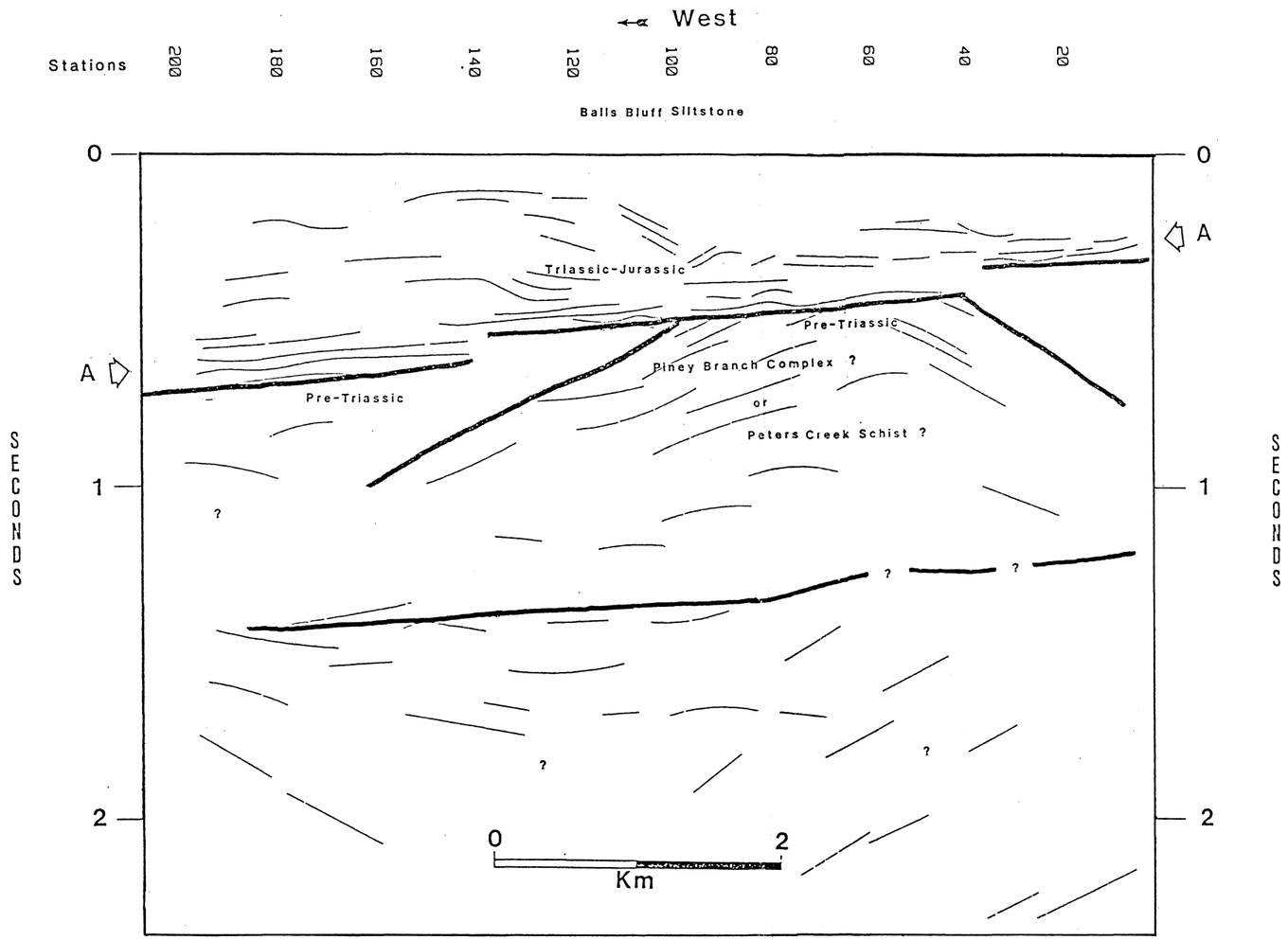

Figure 10. Eastern Culpeper Basin: Line drawing and interpretation with surface geology from Lee (1979).

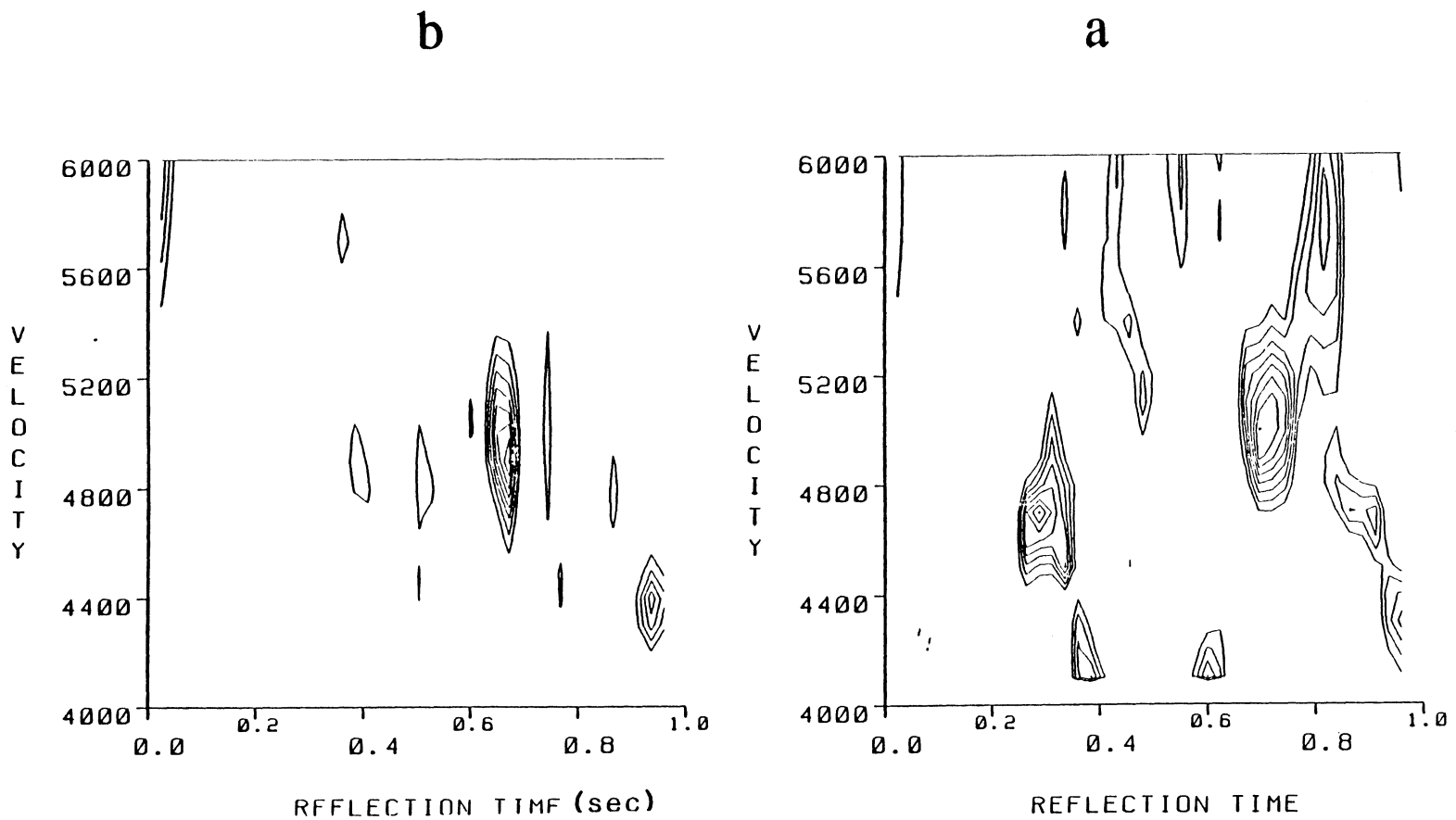

Figure 11. Eastern Culpeper Basin: Velocity spectra from near station 25 (a) and station 175 (b).

unmigrated data (Figure 8) show a possible diffraction from the area below station 145 at 0.6 sec, which collapses after migration (Figure 9); this supports the interpretation of the discontinuity being a result of faulting and also shows that the migration was successful. No apparent diffractions are seen in the area of the interpreted fault below station 40. This lack of clearly defined diffractions is common in the western Culpeper data also, and may be due to the fact that diffractions are obscured by other events, as was demonstrated in modeling the western Culpeper seismic section. High coherency in velocity spectra (Tanner and Koehler, 1969) from this event ("A" in Figure 9) yield RMS velocities which range from 4700 meters per second for the event on the eastern side of the section, to 4900 meters per second on the western side (Figure 11). This implies interval velocities of between 4700-4900 meters per second for the interval between the surface and the reflection.

In general, reflections above 0.0-0.7 sec are relatively weak, in many cases discontinuous, and subhorizontal. These weak reflections extracted indicate low velocity/density contrasts between the various units in this area of the basin. This fits with a geologic description of much of the basin fill as being composed of fluvial deposits (Lindholm, 1979).

Below the large-amplitude, subhorizontal event ("A" in Figure 9) is a group of reflections which delineate an antiformal structure centered near station 60, beginning at 0.4 sec (940 m based on a velocity of 4700 m/sec) and extending to approximately 1.0 sec (2500 m based on a velocity of 5000 m/sec). The limbs of this structure have apparent dips of 25°-35°, and in many cases are truncated by the subhorizontal event from near the bottom of the basin. Thus, the seismic data indicate the presence of a buried, angular unconformity here. A long wavelength aeromagnetic high is centered over this seismic line and can be traced to the eastern border of the basin north-northeast of this line (Johnson and Frolich, 1982; Zietz and others, 1977), where the Piney Branch Complex and the Peters Creek Schist, which contain magnetite and metamorphosed mafic and ultramafic rocks, crop out (Figure 2) (Drake and Morgan, 1981 and 1986). It is possible that this antiformal structure imaged on the seismic line is related to the Piney Branch Complex or the Peters Creek Schist.

The interpretation of this seismic section is shown in Figure 10. The eastern Culpeper seismic profile indicates a much shallower basin (450-1700 m) than that of the western section which may

be as thick as 2500-3000 m. Near the bottom of the basin either a series of highly reflective rock units or a single reflective unit is present ("A" in Figure 9). The bottom of the basin is below this reflection ("A" in Figure 9), and is marked by the presence of an angular unconformity on the eastern side of the profile. The high velocities derived from the velocity spectra and the fact that no single reflection can be attributed to the Triassic pre-Triassic interface again shows poor reflectivity between the basin fill and the surrounding country rock. Reflections within the basin are generally weak and discontinuous, with the exception being the one from near the bottom of the basin. Rock units from near the bottom of the basin, and possibly the floor of the basin, probably contain high-angle faults.

Richmond Basin

The seismic reflection data collected from the Richmond Basin began just east of the basin over the Petersburg Granite, Figure 12 (Goodwin, 1970). The seismic line crosses into the basin, traverses a coal/shale unit and continues over sandstone/siltstone (Goodwin, 1970). From here the seismic line crosses a normal fault and continues over a granodiorite gneiss (Bobyarchick and Glover, 1979), crosses another normal fault, and again enters an area of Mesozoic sediments (coal and shale) (Goodwin, 1970). The seismic line crosses a fourth normal fault leaves the boundary of the basin and traverses pre-Triassic Piedmont rocks(Goodwin, 1970). This westernmost fault is the border fault, and contains mylonite (Bobyarchick and Glover, 1979). The pre-Triassic Piedmont rocks west of the basin are composed of the Sabot Amphibolite overlying the State Farm Gneiss (Poland, 1976; Farrar, 1984).

The recording parameters incorporated in this seismic line are a 12-fold end-off receiver geometry, 350 m near offset, 70 m receiver intervals, and a 22 sec down-sweep of 60-10 Hz. The large near offsets and receiver intervals are in stark contrast to those of the Culpeper Basin seismic profiles. Processing of this line for the purpose of imaging the basin required extra effort in velocity and mute analysis. The velocities were important in that the data exhibited much more NMO with

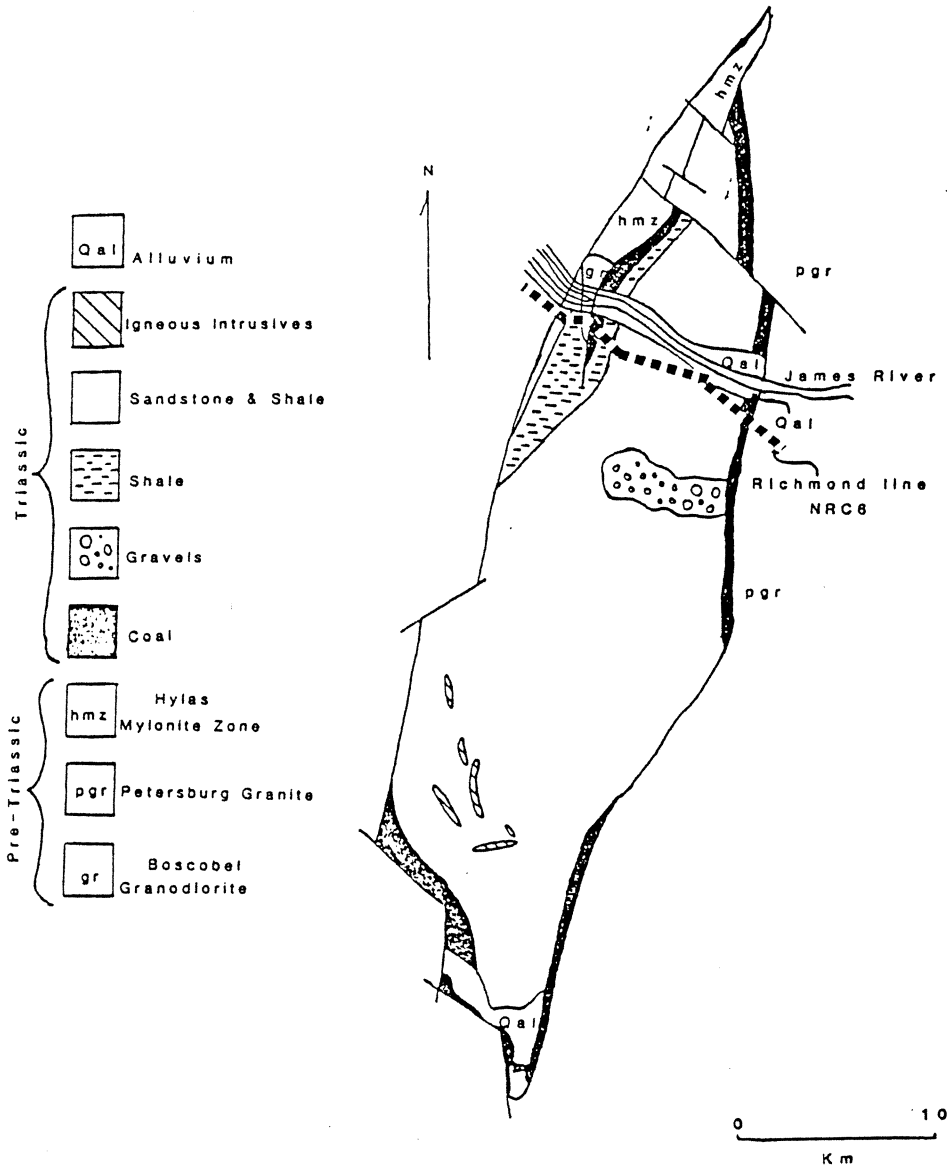

Figure 12. Geology of the Richmond Basin: With location of the seismic survey (labeled 2 in Figure 1) (modified from Roberts, 1928; and Goodwin, 1970).

the presence of the larger offsets than that data in Culpeper. The mute pattern was critical because the mute extended to approximately 0.7 sec, which may be more than half of the depth of the basin.

Because of the problems inherent in processing data designed for deeper reflections to recover shallow reflections, a special technique involving sorting the data into common-offset-range-panels (CORP) was incorporated. This process is intended to study the refracted arrivals to help in determining subsurface geometry, and is based on the delay time method of refraction analysis (Barry, 1967). In general, if the velocities of the refractor are known, the refracted arrivals can be corrected to zero-offset, which is comparable to vertically reflected two-way travel-time for that refracted event. This will give a general geometry and depth of the interface from which those refractions originated, assuming shallow dips of the interface. Note that determination of depth to the refractor is sensitive to dips.

The Richmond data were sorted into CORP's, where each panel contained all of the traces within a specific offset range and were sorted into CMP order. The first panel contained all traces with offsets of 175-595 m. This individual panel can be thought of as an individual seismic line in which the CMP ordered data are 1- to 3-fold and unstacked. Each succeeding CORP contained traces in increasing offset ranges of 419 m. Thus, the second CORP contains all traces in the offset range 596-1015m and the third CORP contains traces in the offset range 1016-1435 m, etc. There are three reasons for grouping the data into offset ranges. If there is a second or a third refraction arriving in the data, this grouping arrangement makes it unlikely that those events will be missed during analysis. The smaller the offset range, the less likely a second or third arrival will be missed. The crooked-line geometry of the seismic line ruled out a chance that large numbers of traces were of the same offset, and by using CORP's a sample from each of the original CMP gathers was assured for most of the CORP's. This grouping also makes possible a method of determining the velocities of the refracted arrivals which is similar to constant velocity analysis (CVA) used on reflection data. Based on the travel-time formula for refracted arrivals $T = T' + (x/v)$, each trace was linearly shifted based on a certain velocity. Note T is the actual arrival time of the refracted arrival, T' is the intercept of the t-x curve with the $x = 0$ axis this is often referred to as the delay time (Barry, 1967), x is the distance from the shot, and v is the velocity of the refracted wave. For ex-

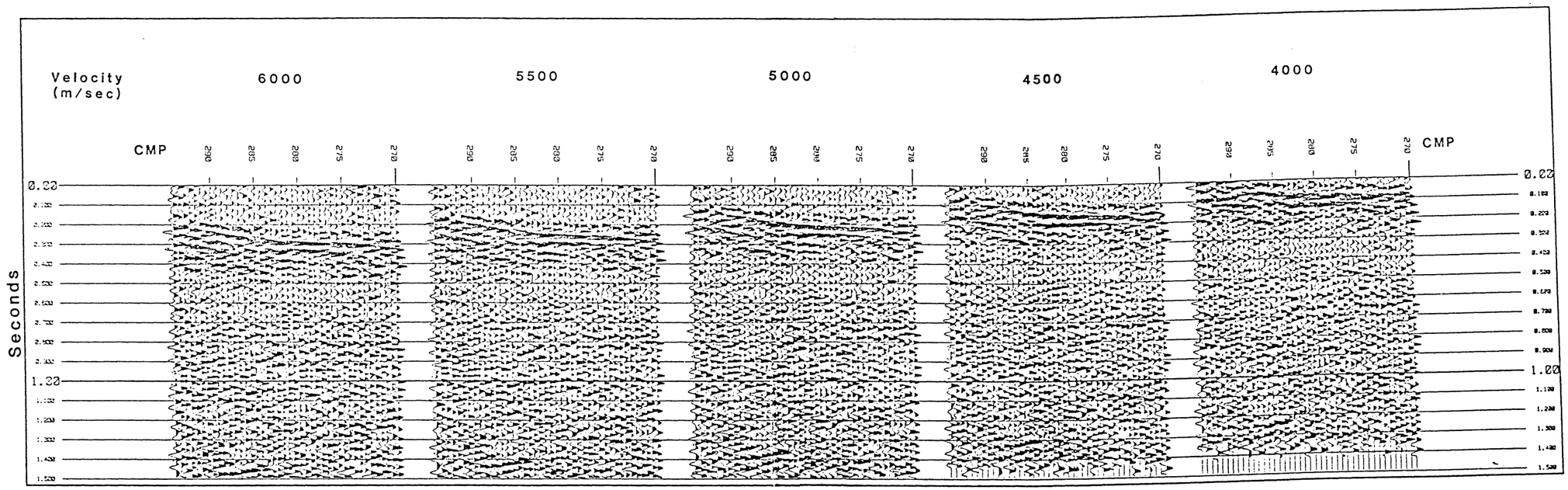

Figure 13. Common offset range panel velocity testing: Portion of CORP **6** adjusted to velocities ranging from 4000-6000 m/sec.

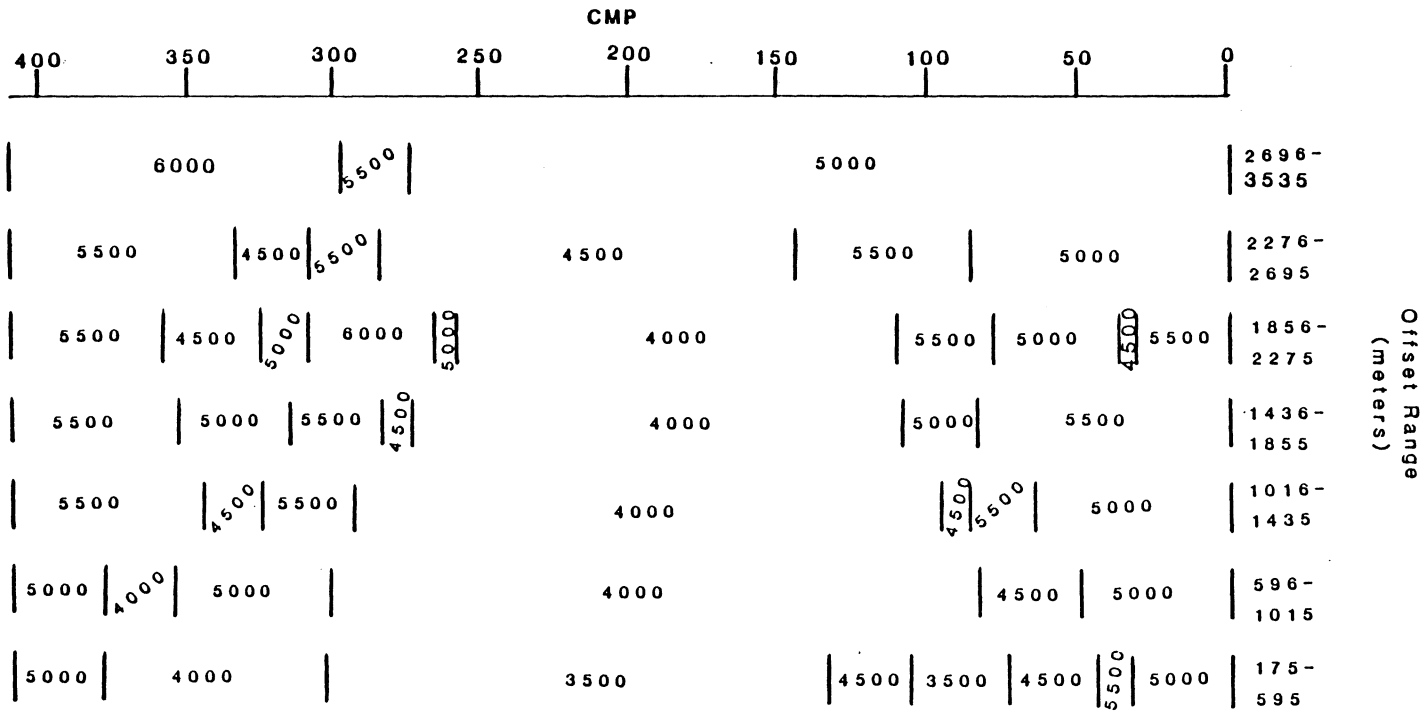

Figure 14. **Richmond Basin velocity function:** Velocity function derived from the CORP velocity analysis: numbers inside the graph are velocities in m/sec.

ample, Figure 13 shows a portion of CORP 6, which contains traces with offset range 2276-2695 m, which have been corrected based on velocities of 4000-6000 m/sec in increments of 500 m/sec. Traces with offsets of 2276 m are shifted 0.455 sec and traces with offsets of 2695 m are shifted 0.539 sec based on a velocity of 5000 m/sec. There is a linear interpolation of the shifts for offsets between these two ends. The data are then examined to see at what velocity the events align themselves most accurately. In Figure 13 the event below CMP's 270-285 appears most continuous at a velocity of 4500-5000 m/sec. The event below CMP's 285-295 appears most coherent at 5500-6000 m/sec.

A velocity function was derived for this data and is shown in Figure 14, where the offset ranges are given on the right-hand side of the graph and CMP location is given at the top. The near offset ranges indicate rapid changes in velocity laterally across the section while the farthest offset indicates a much more continuous lateral velocity function. The velocities were most continuous through the central part of the basin. It is important to note that these are only the apparent velocities, and that the dip of the refraction interface still affects the velocity even with the CMP method employed.

Once the velocities had been determined, the traces were all corrected to zero offset. After applying a low pass filter to enhance the lower frequency refracted arrivals, the 1- to 3-fold data within each panel were stacked to produce zero-offset-panels (ZOP). Stacking the individual CORP's into ZOP's increased S/N. ZOP's 2, 4, and 8 are shown in Figure 15 and lateral changes in the data sets are quite clear. These lateral changes are interpreted to reflect changes in the near-surface geology. In ZOP 2 below stations 180-190 is an antiformal event. This is believed to be a refraction off of the Boscobel Granodiorite (Bobyarchick, 1976; Farrar, 1984). A similarly shaped event can be seen below stations 175-195 in ZOP 4. Again this is believed to be from the granodiorite implying that the body widens with depth. In ZOP 8 no evidence of a similar event can be found in the area below stations 170-200. This is interpreted to indicate a second refraction from a rock unit below the Boscobel Granodiorite is arriving. Similarly, refractions near the surface below stations 195-205 in ZOP 2 are interpreted to be originating in a Triassic rock unit within the small outlier of the main basin. By ZOP 4 this event is replaced by a deeper event which is almost continuous,

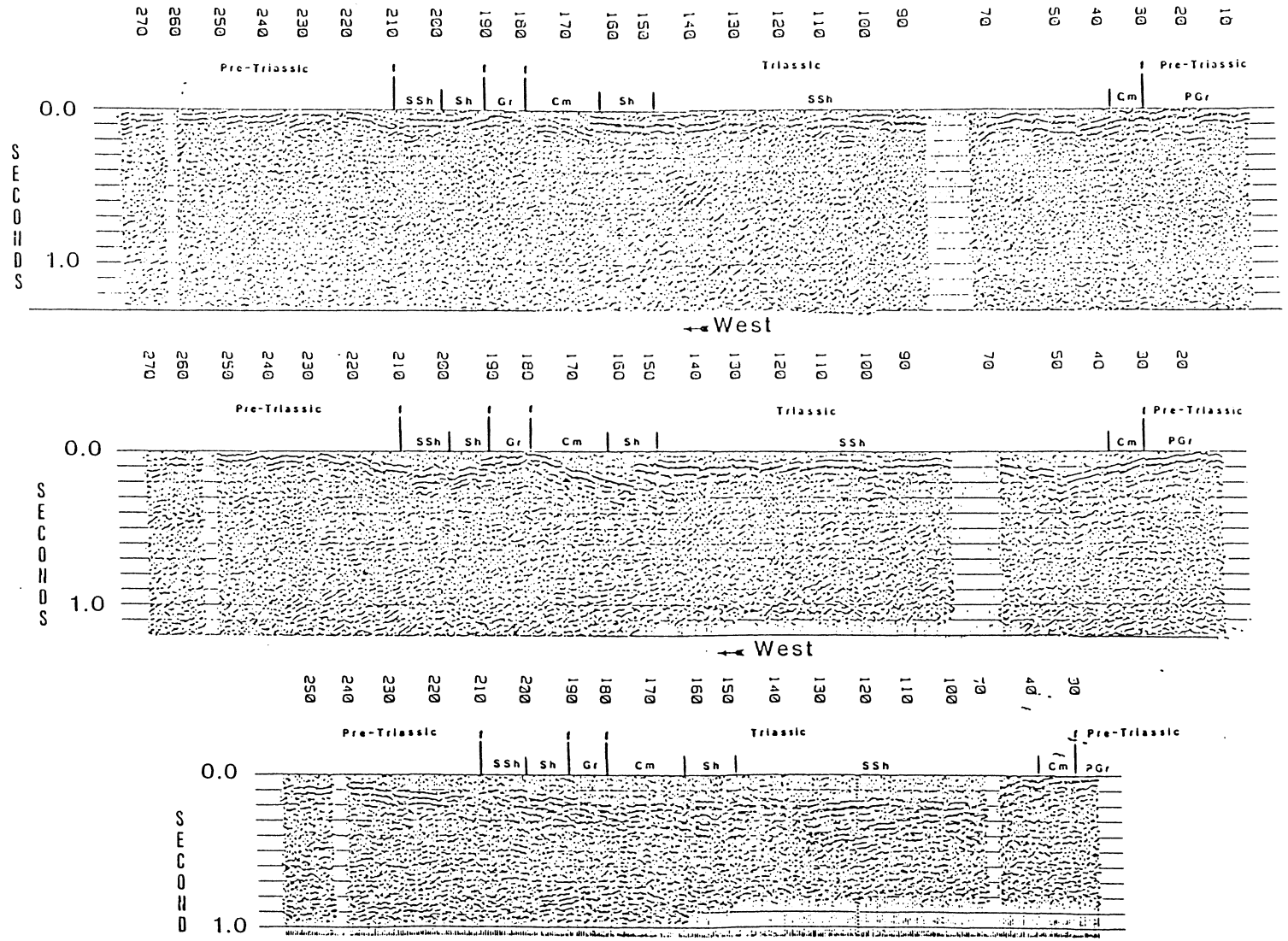

Figure 15. Richmond Basin ZOP: ZOP 2 (offset range 596-1015 m), ZOP 4 (offset range 1436-1855 m), and ZOP 8 (offset range 3116-3535 m). SSh-sandstone and shale, Cm-Coal, Pgr-Petersburg Granite, Gr-Boscobel Granodiorite, Sh-shale, and f-faults (surface geology from Goodwin, 1970; Farrar, 1984).

forming a valley. This may be a refraction from the bottom of this small basin. By ZOP 8 this valley is gone completely.

All of the ZOP data were recombined into the original CMP order, except now the data is 8-fold maximum rather than the original 12-fold. These data were then stacked for a second time to derive a composite of all the individual ZOP's (CZOP). This result is shown in Figure 16. The stacking resulted in quite a bit of smoothing of the data, yet an outline of the basin geometry for the near surface (0.0-0.3 sec) is visible. The discontinuous nature of this refracted data (Figure 16) below stations 30-160 indicates the discontinuous nature of the material within the basin. These data also indicate that the small basin below stations 190-210, west of the major basin, may be no deeper than 500 m, although accurate depth determinations are difficult because of the dipping interfaces. Regardless, it is apparent that refractions are travelling along the base of this shallow outlier. Again, an eastward-dipping event is apparent below the mapped granodiorite below stations 180-190 at 0.2-0.3 sec, and is interpreted to mark the bottom of the Boscobel granodiorite body.

Figure 17 shows an unmigrated section of the Richmond Basin data and Figure 18 shows the same section after time migration. The most notable effect of the migration process here is the movement of the eastward-dipping reflections up and to the west. A large amplitude diffraction below station 140 at 0.8 sec has been collapsed indicating the success of the migration process. Both sections have a low-pass filter with a Hamming ramp designed at 26-39 Hz to enhance the reflection data.

Most of the reflections in the section have apparent eastward dips of 5°-25°. Below stations 0-90 many of these reflections ("A" in Figure 18) are discontinuous on the western side which is interpreted to be related to the basin. Either the eastern edge of the basin is marked by these terminations or the material in the basin above here has distorted the events so much that they are unrecognizable. Recall that to a lesser extent this occurred below the western Culpeper Basin. Mickus and others (1985) estimated a thickness of the basin of approximately 2700 m near the east central portion of this line based on gravity modeling. This would indicate the bottom of the basin should occur somewhere between 1.0-1.2 sec on the seismic section and that reflections below the

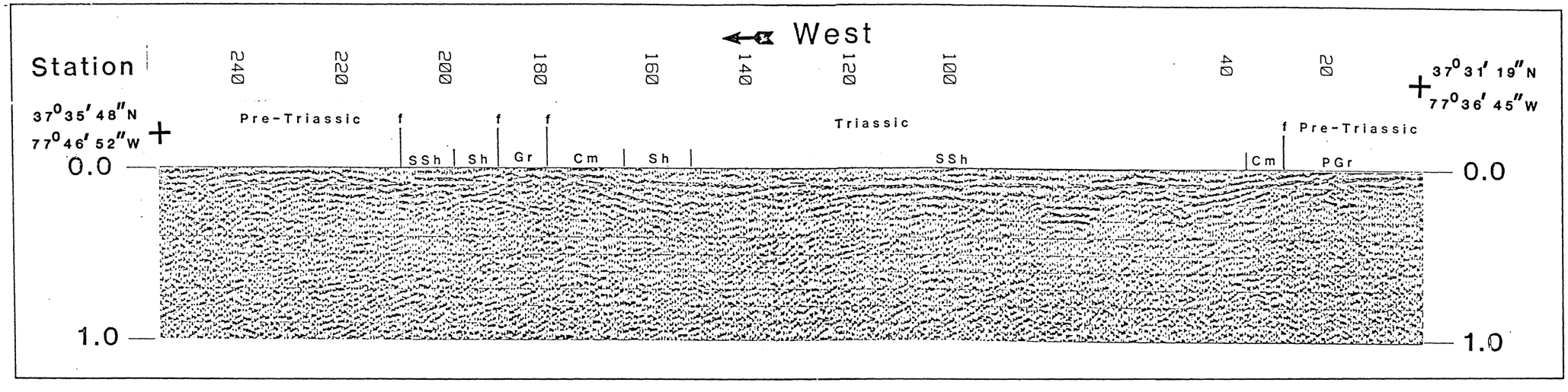

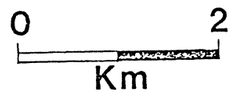

Figure 16. Richmond Basin CZOP: SSh-sandstone and shale, Sh-Shale, Cm-coal, Pgr-Petersberg granite, Gr-Boscobel Granodiorite, and f-faults (surface geology from Goodwin, 1970; Farrar, 1984).

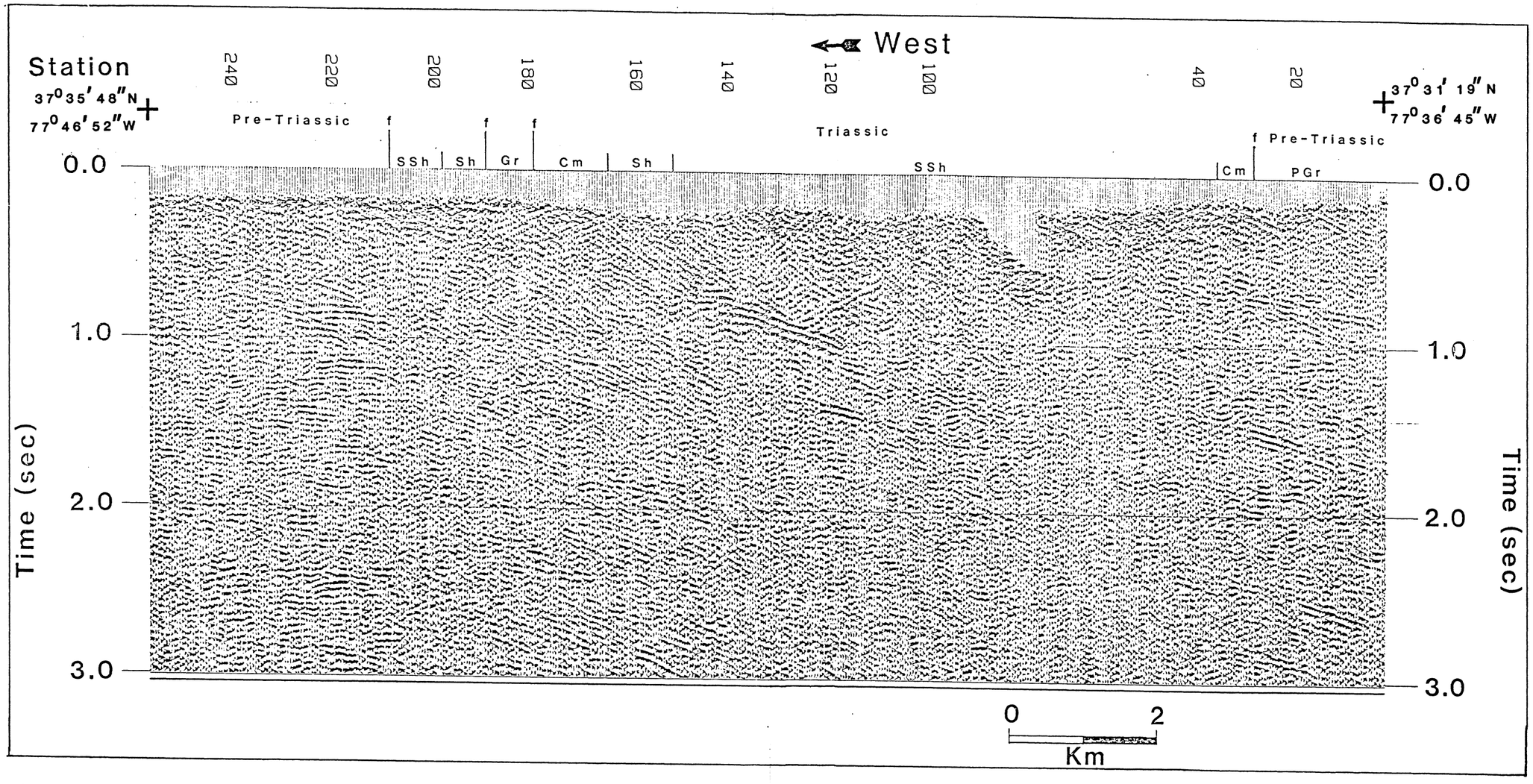

Figure 17. Richmond Basin: Unmigrated section; SSh-sandstone and shale, Sh-shale, Cm-Coal, PGr-Petersberg Granite, Gr-Boscebel Granodiorite, and f-faults (surface geology from Goodwin, 1970; Farrar, 1984).

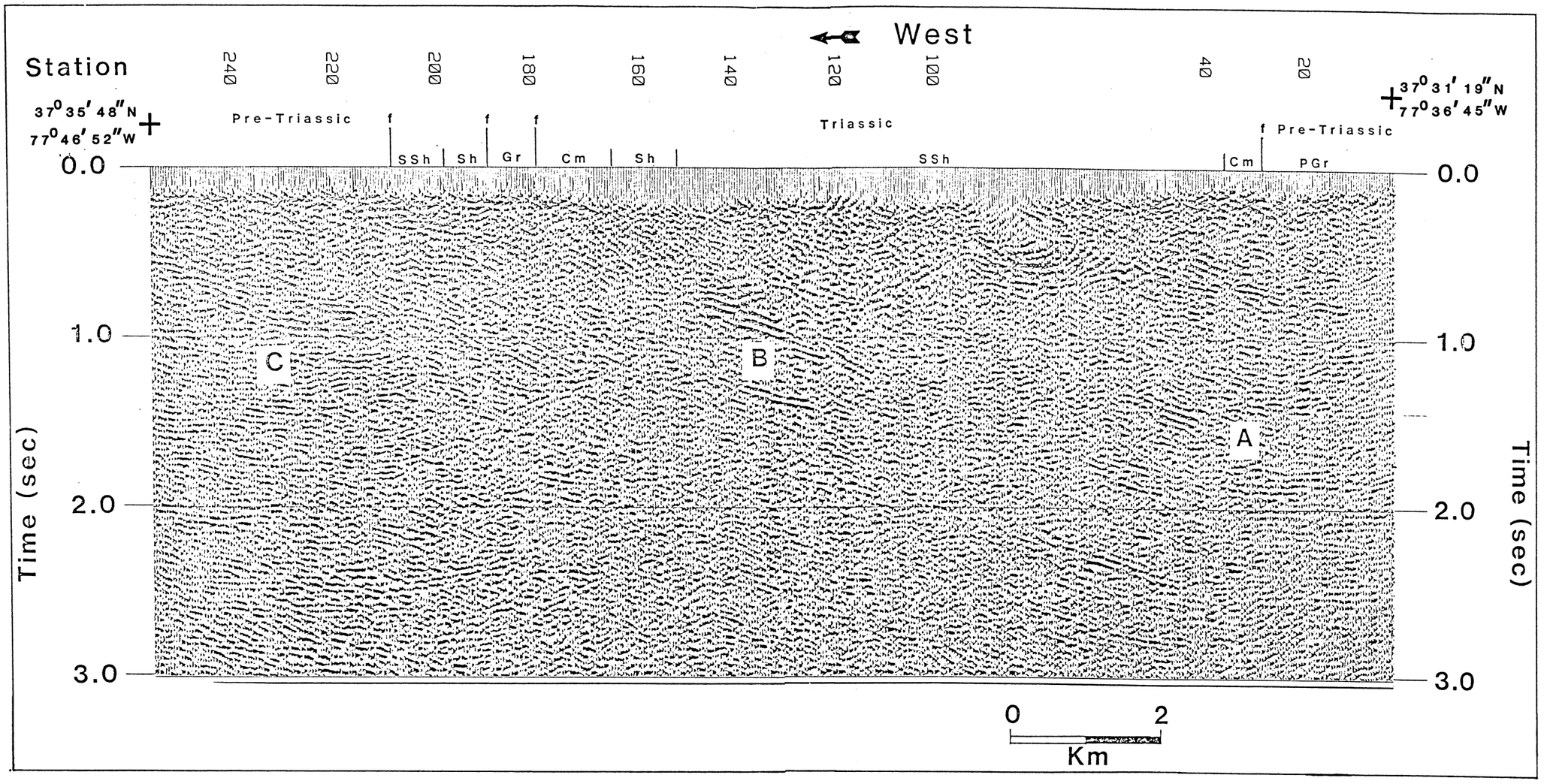

Figure 18. Richmond Basin: Time migrated section; SSh-sandstone and shale, Sh-shale, Cm-coal measures, Pgr-Petersberg Granite, Gr-Boscebel Granodiorite, and f-faults (surface geology from Goodwin, 1970; Farrar, 1984).

basin are being distorted when they travel through the basin. This is probably the case as few of the reflections on either side have amplitudes as large as those in the western Culpeper section, and little distortions of these events could easily obscure them.

Figure 19 shows a line drawing along with a possible interpretation. Below station 140 at 0.6-1.0 seconds is the largest amplitude event on the section ("B" in Figure 18). Below this at approximately 1.3-1.5 sec is another short, large-amplitude event. Prior to migration, the event at 0.6-1.0 sec proved to be partly from a diffraction phenomenon (Figure 17), is interpreted to be due to a fault. The large-amplitude discontinuous reflection may be from outside of the basin and is terminated on the eastern end below station 120 at 1.1 sec by what may be another fault marking the start of more Triassic material to the east (Figure 19).

Subhorizontal and eastward-dipping reflections west of the basin ("C" in Figure 18), and also those below 1.5-2.0 sec throughout the section, have several possible origins. They may be related to the Sabot Amphibolite or the State Farm Gneiss which crop out west of the basin (Reilly, 1980; Farrar, 1984). Some of them may be related to the Hylas Zone, which is a mylonite and forms the border fault of the basin (Bobyarchick and Glover, 1979).

Reflections from within the basin are not recognizable in this data set, and none of the reflections can be directly attributed to the bottom of the basin indicating that higher lateral resolution methods are needed to extract these reflections, which seems to be the general case for the other basins also. The refraction data indicate discontinuous faulted and folded units within the basin. The success of the refraction study indicates that this may be a good method of exploring these and similar basins. If refraction analysis is used in conjunction with reflection data, larger offsets are recommended.

One reason for the poor quality of the data may be poor velocity contrasts between the Triassic rock units within the basin and the pre-Triassic rock units surrounding the basin. Other reasons include complex and discontinuous structures as indicated by the refraction analyses.

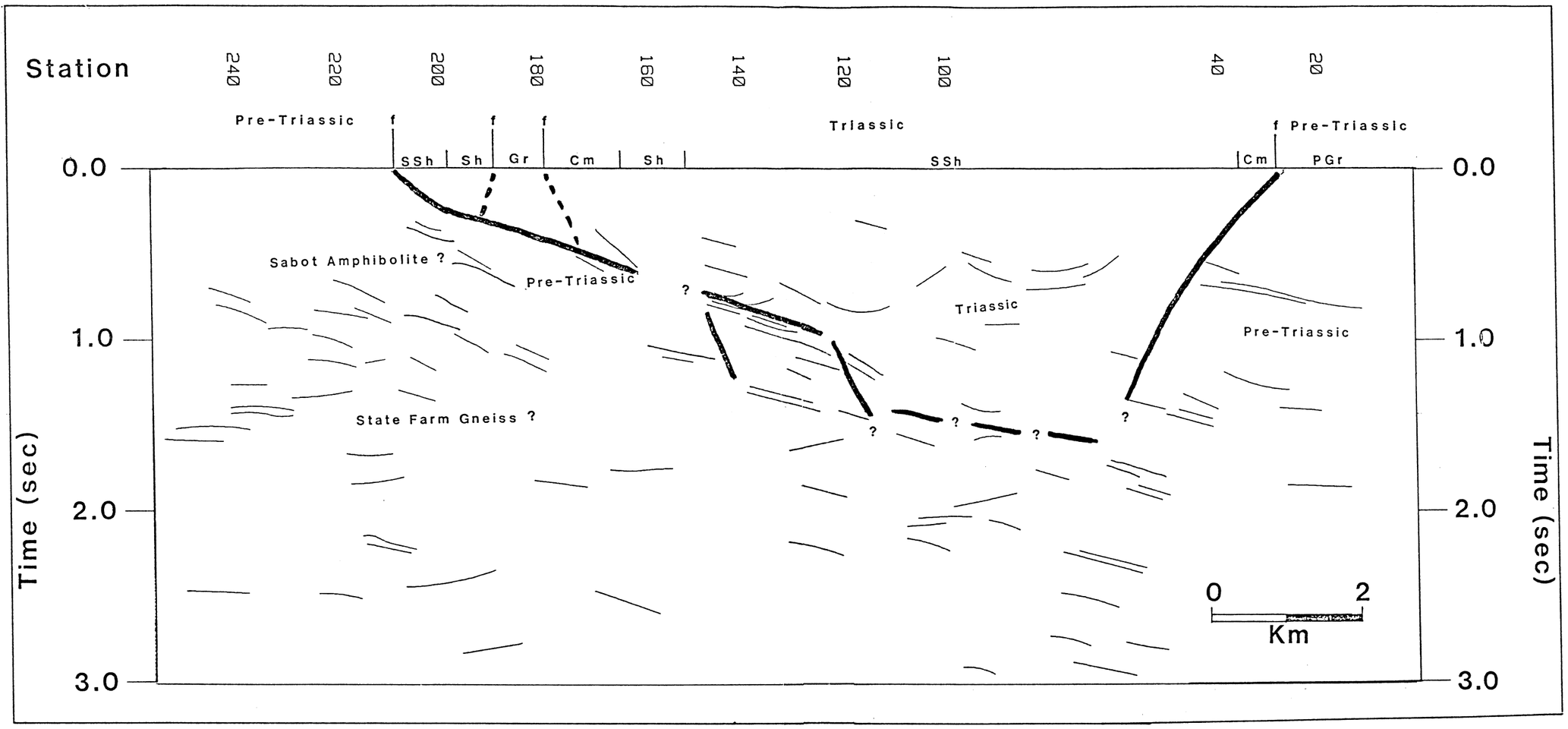

Figure 19. Richmond Basin: Line drawing and interpretation, SSh-sandstone and shale Sh-shale, Cm-coal, Pgr-Petersberg Granite, Gr-Boscobel Granodiorite, and f-faults (surface geology from Goodwin, 1970; Reilly, 1980; and Farrar, 1984)

Scottsville Basin

The Scottsville basin is composed of poorly sorted red sand/siltstone and fanglomerates (Nelson, 1962), and is shown along with the general location of the seismic line in Figure 20. The seismic line begins approximately 320 m west of the eastern side of the basin (Nelson, 1962), traverses the sedimentary strata, then crosses into the Evington Group (Glover, in preparation). for a short distance (Figure 20). Further west of the seismic line, the Catoctin Formation (metamorphosed basalt flows interbedded with sedimentary strata) overlies the Swift Run Formation (quartzite, slate, and greenstone) (Nelson, 1962).

The data collected from the Scottsville Basin had recording parameters identical to those used in the Culpeper Basin except for the sweep, which was a 16 sec downsweep of 80-10 Hz, and a 70 m near offset. Processing of the data followed the same pattern as the Culpeper lines. These data were deconvolved with a predictive deconvolution filter with a gap of 20 msec, and a filter length of 70 msec. The short offsets made CORP and ZOP analysis of the data inappropriate for defining geometries. However, cursory analysis of the refractions using CORP analysis across the section yield velocities of 5000-5300 m/sec near the surface within the basin, and 5500 m/sec near the surface outside of the basin, which may result in poor reflectivity to define the geometry of the basin. Note that the Scottsville data is recorded with a split-spread receiver geometry and this should act as method of averaging the apparent velocities and remove much of the problems in determining velocity associated associated with dipping refractors. Therefore, the velocities of 5000-5300 are considered to be representative of the actual velocities.

Figure 21 shows the unmigrated section from the Scottsville area and Figure 22 shows the same section after time migration. Because of the wide bandwidth employed in the collection of the data, numerous low-pass, band-pass, and high-pass filters were tested on the data to determine which range of frequencies most successfully indicated the geometry of the basin. A band-pass filter with Hamming-designed ramps on the low end of 10-14 Hz and on the high end of 40-60 Hz gave the best results. Migration improved the S/N and moved many of the dipping reflections around.

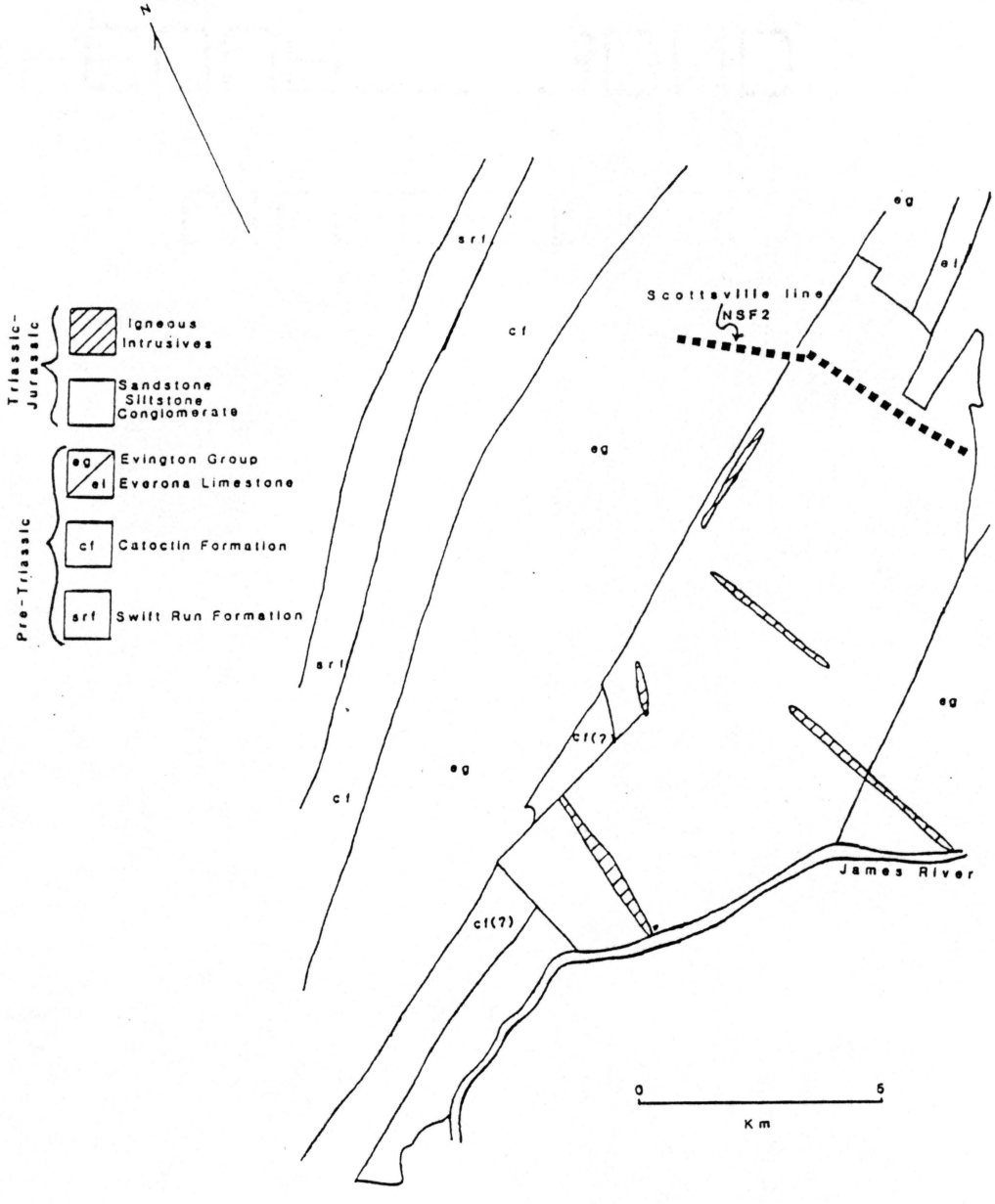

Figure 20. Geology of the Scottsville Basin: with location of the seismic line (labeled 3 in Figure 1) (surface geology from Nelson, 1962; Glover and others, in preparation).

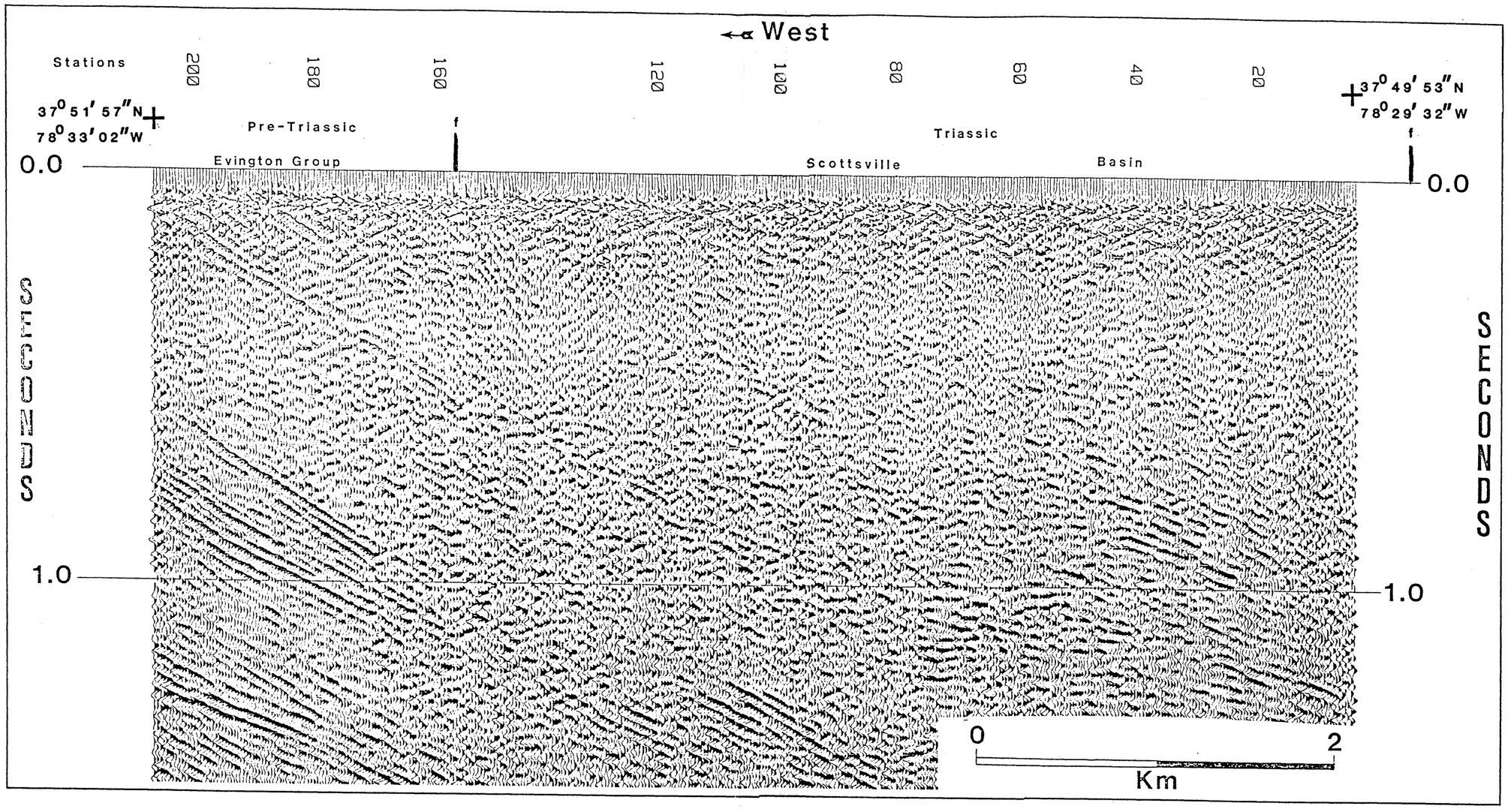

Figure 21. Scottsville Basin: Unmigrated section (surface geology from Nelson, 1962; Glover and others in preparation).

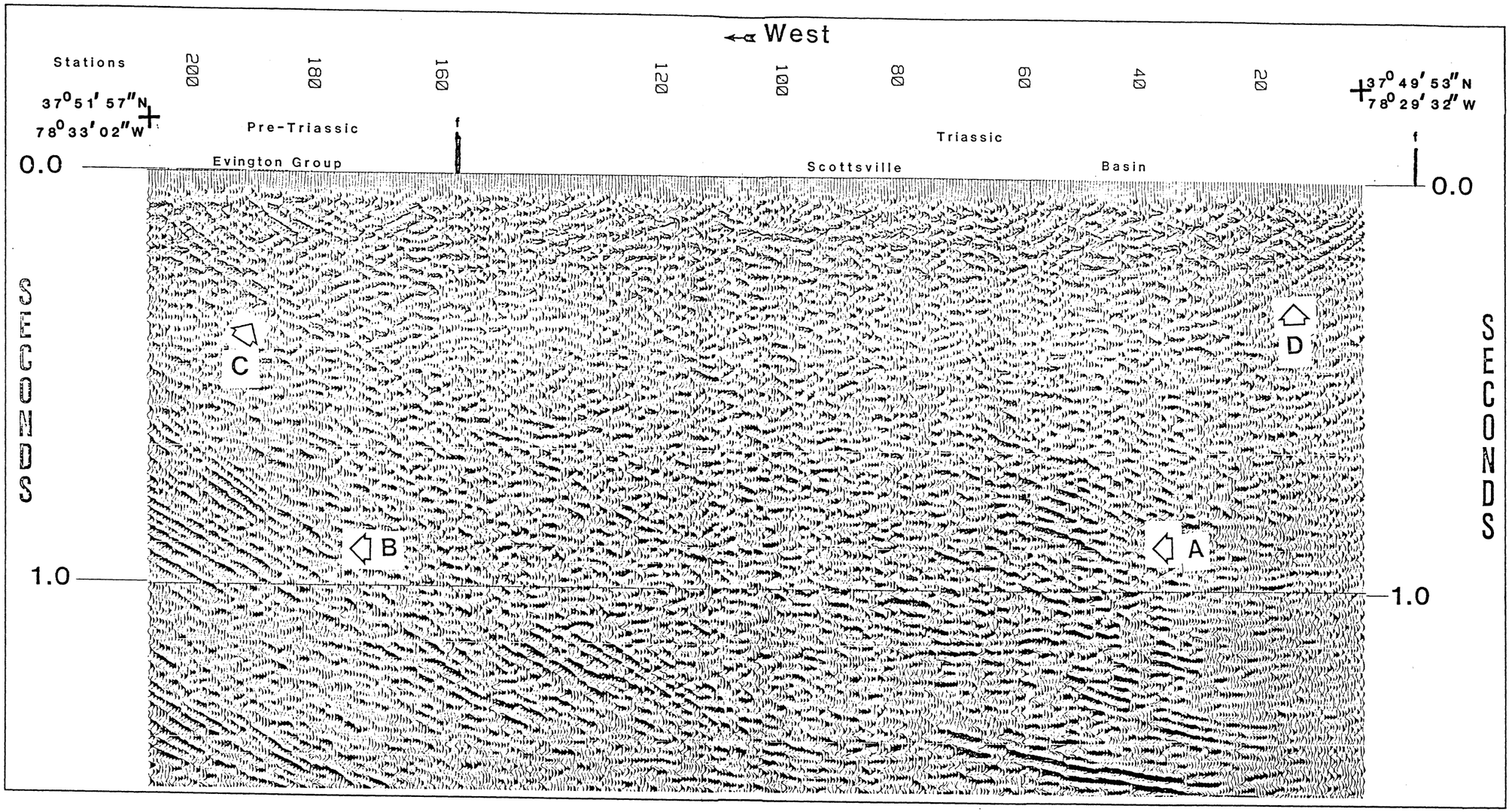

Figure 22. Scottsville Basin: Time-migrated section (surface geology from Nelson, 1962; Glover and others in preparation).

In particular, reflections in the unmigrated section (Figure 21) below stations 160-205 at 0.5-1.5 sec are pushed up and to the west and in many cases are pushed out of the plane of the section ("B" in Figure 22).

Figure 23 shows a line drawing and interpretation which are based on the migrated section. The data from 0.0-1.0 sec in general are filled with relatively weak and discontinuous reflections, with exceptions occurring below stations 40-60 at 0.6-1.0 sec ("A" in Figure 22) and below stations 180-205 at 0.6-1.0 sec ("B" in Figure 22). One event which may indicate the location of the bottom of the basin begins at 0.1 sec on the far eastern edge of the section ("D" in Figure 22). This event has an apparent westward dip of 30°-35° and gradually flattens as it is traced to below stations 20-25 at 0.2-0.3 sec where it becomes discontinuous. Extrapolating this event to the surface (Figure 22) indicates that it correlates with the area just west of the eastern edge of the basin. The multilobe nature of the reflected wavelet combined with the correlation implies that the reflection originated from a rock unit or units within the basin. The bottom of the reflected wavelet may indicate the general location of the floor of the basin.

Below stations 40-60 at 0.5-1.0 sec are a group of relatively large-amplitude reflections ("A" in Figure 22); the termination of these events may imply the location of the eastern edge of the basin. At least one other possible explanation for the abrupt end of these reflections can be extrapolated from the modeling done in the western Culpeper seismic line. If there is complex structure above the area, then it is possible that reflections from below will be broken up. But, while it is possible that this is the case the drastic change in character of the reflections indicates a geological break best explained by the presence of the Scottsville Basin to the west (Figure 23). It is improbable that the basin extends below 1.0-1.1 sec (2650-2915 m) because of the presence of a reflection ("C" in Figure 22) which can be followed discontinuously from the western edge of the section at 0.1 sec along a curved path to below stations 60-80 at 1.0-1.1 sec.

The western edge of the basin is indicated by a change in character of the reflections as was the case in the eastern side of the section. Just to the west of stations 150-160 are a group of relatively large amplitude reflections at 0.0-0.5 sec. These reflections come to an abrupt end below stations

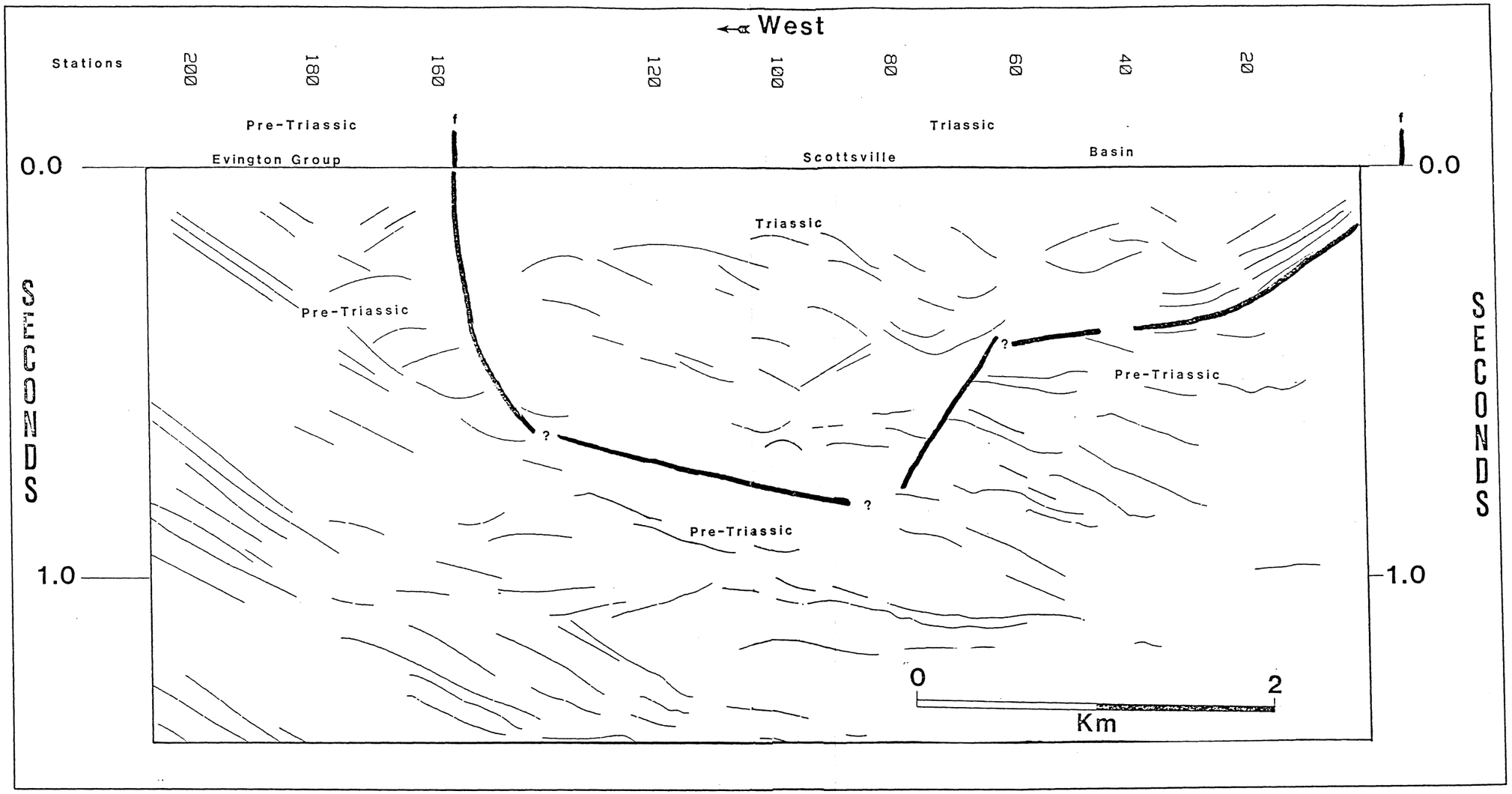

Figure 23. Scottsville Basin: Line drawing and interpretation derived from the migrated section; surface geology from Nelson, (1962); Glover and others in preparation.

150-160 and this is interpreted to be the location of the western side of the basin. This side may continue to a time of 0.4-0.6 sec (1060-1600 m).

Reflections seen on the western side of the section at 0.5-1.5 sec with apparent dips of 35°-50° may have originated from the Catoctin Formation or the Swift Run Formation which crop out west of the basin (Nelson, 1962). These and deeper reflections from this line have been interpreted in more detail by Glover and others (in preparation).

As with the Richmond and the eastern Culpeper seismic data sets, no clear reflections marking the bottom of the basin are present in the Scottsville. The reason for this in the Scottsville is much more apparent when one considers the high velocities (5000-5300 m/sec) derived from the refraction data in the Scottsville which may result in low reflection coefficients at the Triassic pre-Triassic interface. These high velocities also give the basin a relatively shallow appearance in the seismic profile (Figure 22); however, 0.7 sec in two-way travel-time converts to 1750 m in depth. Another feature becoming more and more common with each new seismic section introduced is the lack of diffractions marking boundaries. Modeling from the western Culpeper line indicated that complex structures were causing numerous diffractions to cancel one another. This may be the case here also.

Toano Basin

The seismic reflection data collected over the Atlantic Coastal plain (I-64) for the U. S. Geological Survey, by Geophysical Service Inc., was initially reprocessed for deep reflections (Pratt and others in preparation). The data were included here after initial results indicated a basin structure of probable Triassic-Jurassic age. A well drilled north of this seismic line near the town of West Point (Figure 24) hit possible late-Jurassic rocks at near 300 m and Triassic rocks at a depth of 380-500 m below the surface of the Coastal Plain (Johnson, 1975; Brown and others , 1972). Note that with a velocity of 2000 m/sec the two-way travel-time for an event at 300 m would be 0.3 sec. Other Mesozoic basins have been interpreted to be present below the Coastal Plain from similar

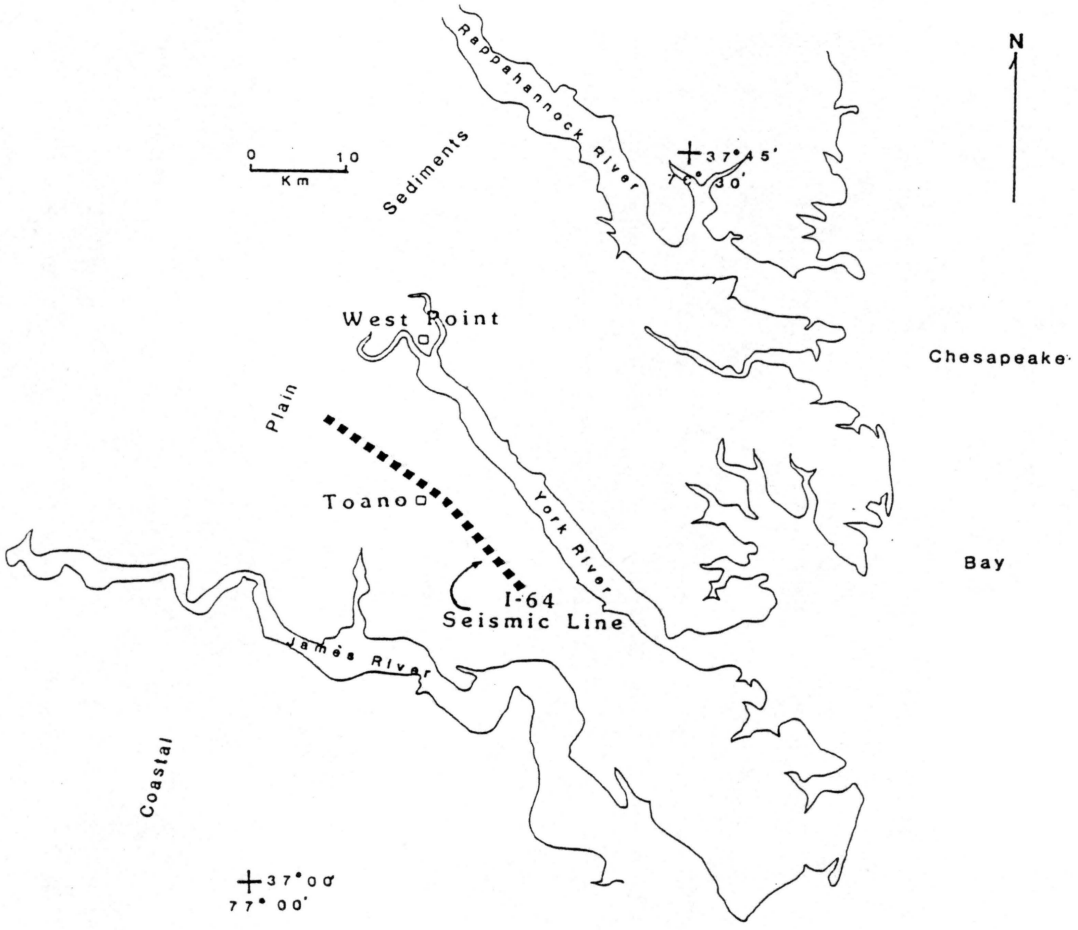

Figure 24. Toano Basin: Location of the Toano Basin seismic line (labeled 4 in Figure 1) (modified from Johnson, 1973 and 1975).

well data (Brown and others, 1972; Johnson, 1975; Petersen, 1984). The portion of the seismic line discussed here is between the York and James Rivers and runs just north of the town of Toano (Figure 24). The general area also contains a low Bouguer gravity anomaly which is elongate and trends in a north-north-westerly direction (Johnson, 1973 and 1975), although no gravity anomalies are observed in the Culpeper and Scottsville basins, where they may be obscured by larger regional gravity gradients.

The data were acquired using essentially the same receiver intervals and near offsets as the Richmond seismic line: however, the recording configuration is split-spread, which cuts the far offset to roughly half of that in the Richmond, with the farthest offsets being approximately 1800 m. The near offset for these data was only 201 m compared to the 350 m for the data from the Richmond Basin. The data were collected with a 10 sec sweep of 14-56 Hz.

Offsets were far enough to enable meaningful CORP and ZOP analysis of the refractions to help image the geometry of the basin, as was done in the Richmond data. In this case, the first CORP contained traces from the offset range 190-630. The second CORP contained all traces with offsets 604-1017, and these are incremented by 413 m each time to derive 6 CORP's.

A velocity analysis, as was described in the Richmond section was performed, and the results are shown in Figure 25. As with the Richmond data, the higher velocities appear to mark the location of the eastern and western edges of the basin below CMP's 6050 and 6720 in the near offset CORP's and below stations 6100 and 6750 in the CORP's with the larger offsets. These velocities were more difficult to determine than those of the Richmond Basin primarily because these data have a lower S/N than the data from the Richmond Basin. Data in the offset range 872-1140 (CORP 3) indicate the clearest picture of the velocity function and shows rapid lateral changes in velocity which may indicate rapid changes in rock type.

The results of these CORP and ZOP analyses are not as clear as those from the Richmond Basin. ZOP 5, which contains traces with offsets of 1410-1678 m, is shown in Figure 26. This panel provided the best resolution of all of the ZOP's. The edges of the basin are indicated to be below station 3200-3240 on the western side and below stations 3520-3550 on the eastern side of the section. At these places the refraction data in ZOP 5 provide a much clearer image of the basin

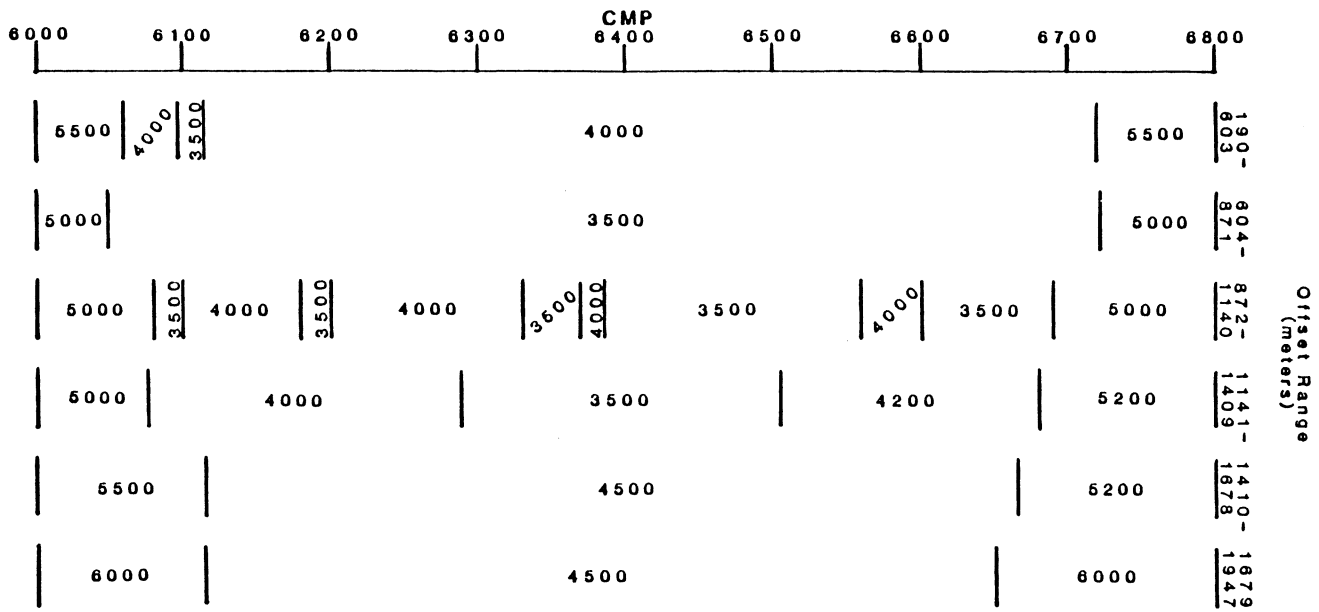

Figure 25. Toano Basin: Velocities derived from CORP analysis; numbers within the graph are velocities in m/sec.

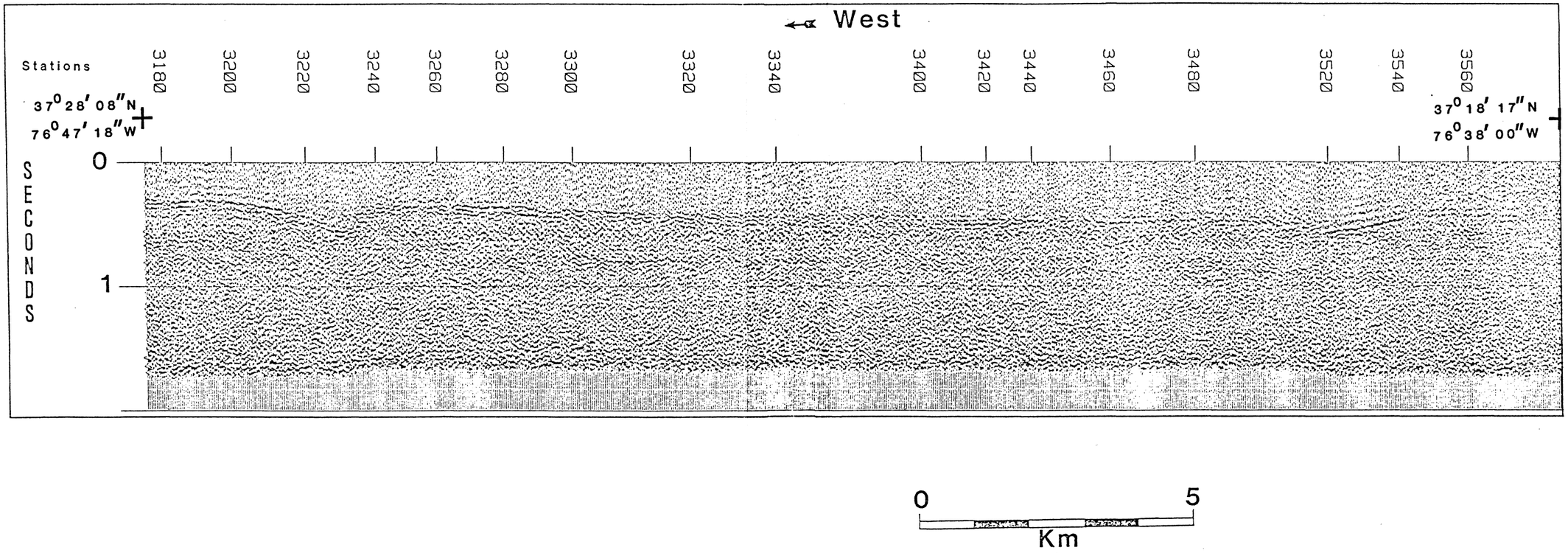

Figure 26. Toano Basin: ZOP 5 containing traces from offset range 1410-1678 after correction for given velocities and stacking.

structure than the reflection data. The subhorizontal refraction along the western side of the section at 0.3 sec turns downward below stations 3200-3230 and acquires an apparent dip of 10°-20° east. Along the eastern side of the section, below stations 3540-3580 a faint image of a subhorizontal event can be seen at near 0.4 sec (Figure 26). Below station 3540 this event turns downward and acquires an apparent dip of 10°-20° west. These two events mark the edges of the basin indicating the basin here has an apparent width of approximately 26 Km.

The ZOP 5 is comparable to the reflection data, both unmigrated and migrated, which can be seen in Figure 27 and Figure 28, respectively. Migration did not improve these data appreciably. In general, the S/N is similar on both sections and dipping events have not been adjusted significantly. As with the previous data, these data were filtered to enhance the reflections from the area of the basin. The data were deconvolved, which removed a ringy appearance to the original data. This filter was designed with a gap of 30 ms and a filter length of 104 ms.

The most prominent reflection on the section is subhorizontal and occurs at 0.3 sec on the western end of the section and at 0.4 sec on the eastern end of the section (Figure 28). This is interpreted to originate from the bottom of the Coastal Plain sediments. Below station 3210 at 0.3 sec is a gentle (10°-20°) eastward-dipping event which can be followed to below station 3280 at near 1.0 sec ("A" in Figure 28). Below station 3540 at approximately 0.4 sec is the antithesis to the previously described event dipping 10°-20° westward ("B" in Figure 28). This event can be followed to below station 3420 at 1.4 sec. The seismic reflection data does not resolve whether these reflections originated from Triassic pre-Triassic interface. None of the previous data in this study resolve good reflections from this interface; however, data from the Newark Basin do provide reflections from the Triassic pre-Triassic interface which are due to a high velocity dolomite on the pre-Triassic side of the border fault (D'Angelo, 1985; Ratcliffe and others, 1986). Thus, while the data in this study indicate that reflections from the Triassic pre-Triassic interface are too weak to be resolved on the seismic profile, this can not rule out the fact that the reflections on the Toano Basin seismic data ("A" and "B" in Figure 28) may have originated from the borders of this basin. Below stations 3340-3450 at 0.4-0.8 sec is a group of reflections forming a curve, which is concave upward. If the lignite recovered from the drill-hole near the town of West Point (Brown and others,

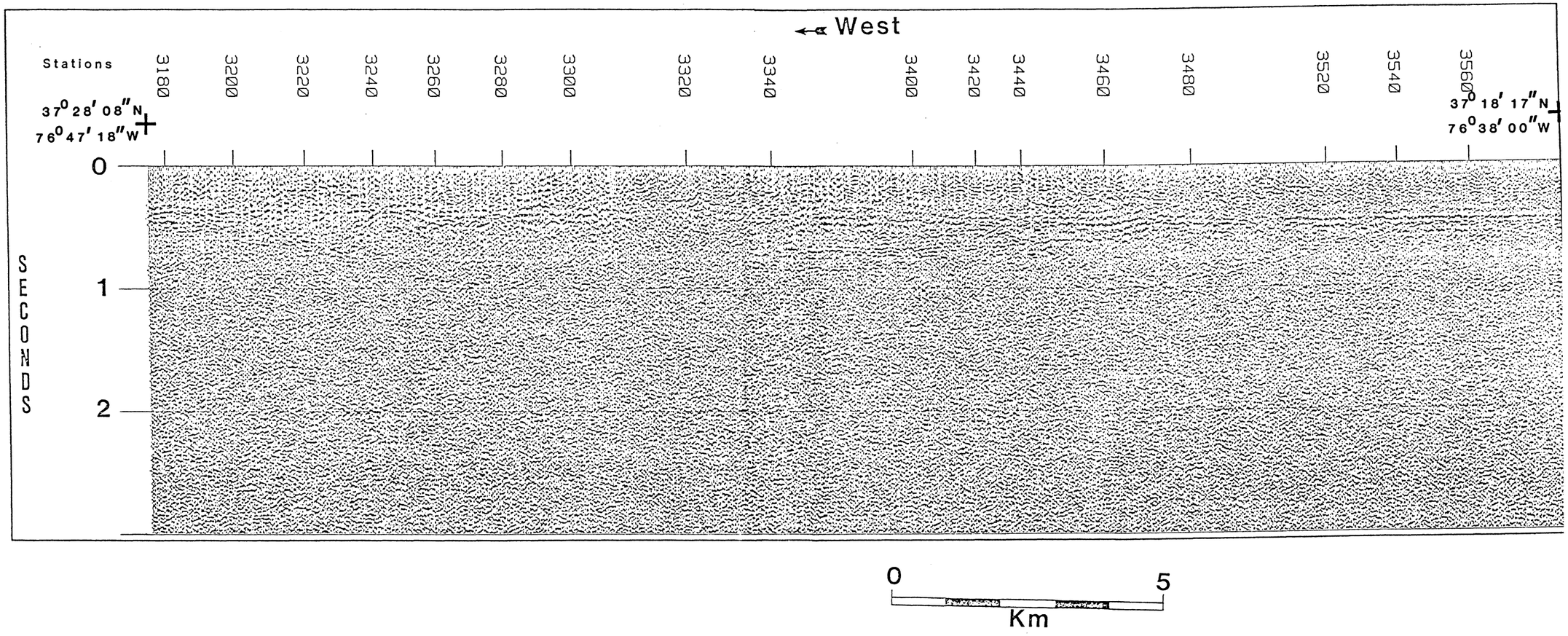

Figure 27. Toano Basin: Unmigrated seismic reflection section.

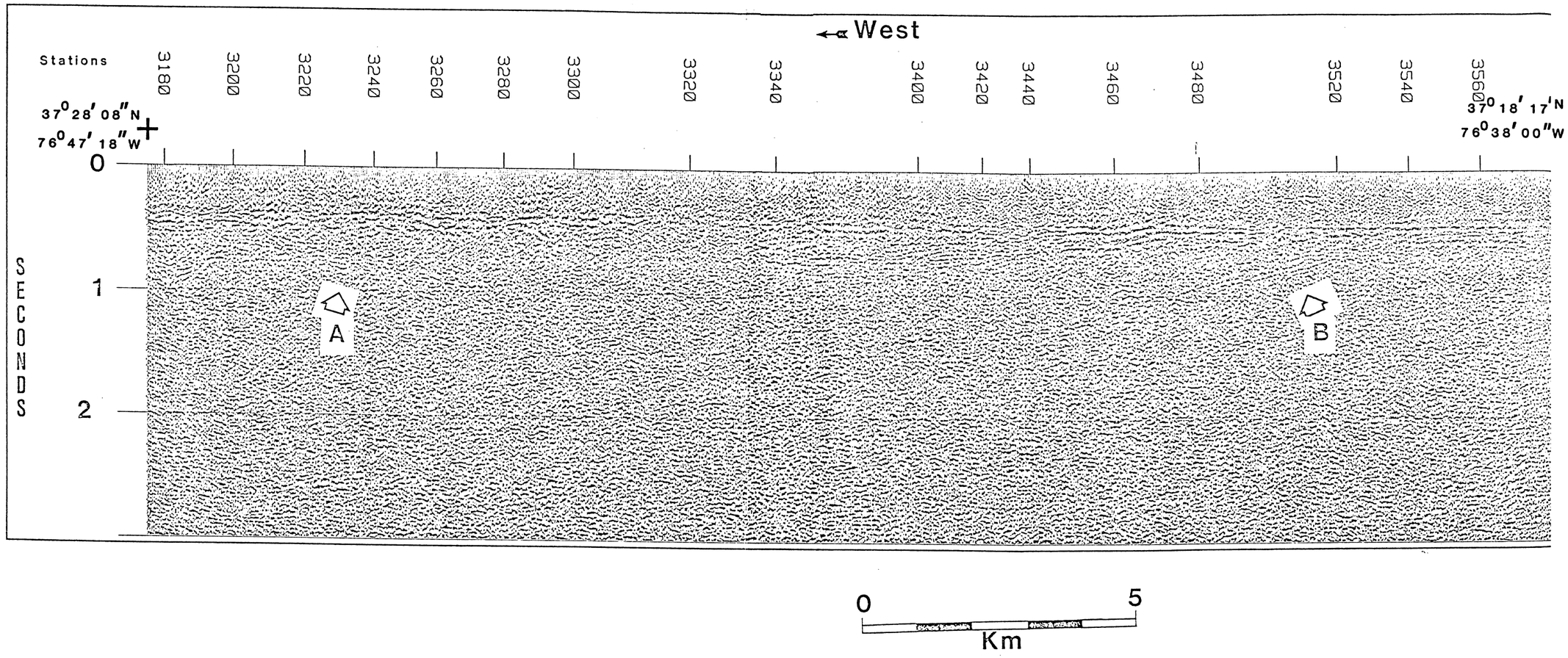

Figure 28. Toano Basin: Time migrated seismic reflection section.

1972) is from the basin imaged in the seismic profile than it is probable that these reflections below stations 3340-3450 are from similar rock units. The low velocity of coal (related to lignite) (Cordier, 1985) would provide a good reflection coefficient in the same manner as the high velocity of basalt did in the western Culpeper section (Figure 4).

The general interpretation for the geometry of this basin (Figure 29) is that it is a much more symmetrical basin than the Culpeper, Scottsville, or the Richmond Basins. Although the reflections marking the edges of the basin ("A" and "B" in Figure 28) are interpreted to indicate a general location for the bottom of the basin, they are not believed to have originated from the bottom of the basin. extrapolating these reflections to depth implies a possible thickness of the basin of 3500-4000 m. This thickness is tentative because of the poor quality of the data. The changing amplitude of the arrivals from both the reflection data (Figure 28) and the CZOP data (Figure 26) directly over the basin indicate possible lateral changing rock types.

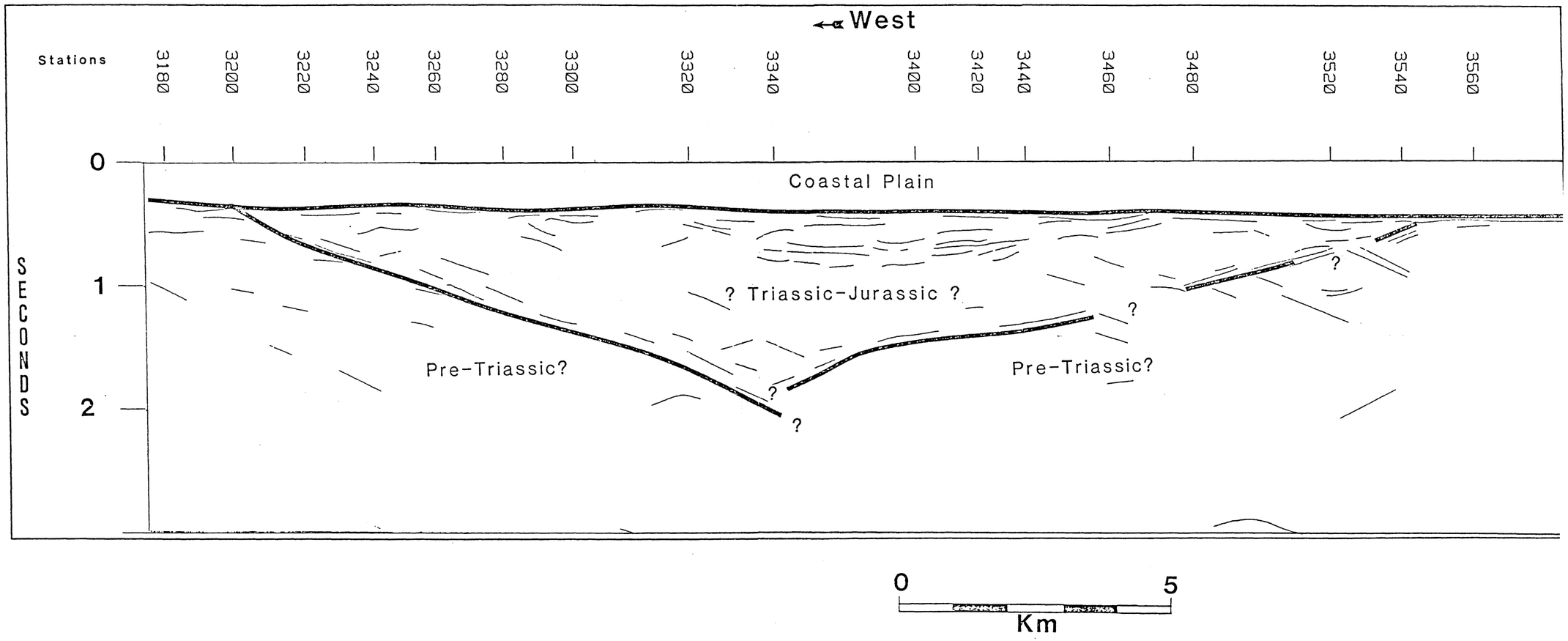

Figure 29. Toano Basin: Line drawing and general interpretation.

Discussion

Studies of the seismic data from the Early Mesozoic basins of Virginia indicate that the structure of the basins generally combined with low velocity/density contrasts within the basins and between the basin and the surrounding country rock are the primary reasons for poor quality of the data, as opposed to the idea that the recording parameters are the primary reason for this poor quality data. The two seismic profiles from the Culpeper Basin incorporated short offsets (34.5 m), and these resulted in clear images of the basin. This might imply that short offsets are the key to designing recording parameters; however, the short offsets (34.5 m) incorporated in the Scottsville data did not adequately image that basin, even with the added frequency content (80-10 Hz). Even though the data from the Richmond and the Toano basins were collected with larger offsets the deeper data, which should have been only slightly affected by the stretching caused by NMO corrections and not affected by the mute at all, are still of a poor quality. Velocities derived from the CORP analysis of the refractions and analysis of the shot data range from 4500-5300 m/sec for the Triassic-Jurassic rock units while those of the surrounding country rock range from 5000-6000 m/sec. In many cases this may provide only small reflection coefficients (0.02). If the basin contains basalt flows, then a large enough reflection coefficient was present to produce clear reflections as was seen in the western Culpeper line. It is possible that other anomalous rock units are the reason for reflections from within other basins, such as possibly coal or lignite as suggested for the

Toano basin from drill samples north of the seismic line (Brown and others, 1972). The complex structure seen in the western Culpeper line distorted reflections from below the basin as was demonstrated by modeling. Similar complex structures in other basins may be the reason for obscuring reflections from the bottom of the basins and below, such as is seen in the Richmond and the Scottsville basins.

One very successful method of analyzing the basins was revealed when the refracted arrivals of the data from the Richmond and the Toano Basins were studied by arranging the data into CORP and ZOP gathers. The analysis of the CORP data allowed the apparent velocities of the refracted arrivals to be resolved to approximately 500 m/sec. If the data are recorded with split-spread receiver geometry, and the the CORP analysis is carried out with each offset range sorted into CMP gathers, this should act as an averaging technique, and the velocities obtained should not be as susceptible to dipping interfaces. Both ZOP analyses delineated the geometry of the shallow portions of these basins better than the reflection data. This method can be combined with the information derived from the reflection data to enhance interpretation of the near surface features. If this method is employed in future studies from these and similar basins it would be useful to obtain larger offset records than those obtained from these seismic profiles.

Comparison of the various seismic reflection profiles indicate many similarities and differences in the data. None of the seismic sections exhibited reflections which could be directly attributed to a Triassic pre-Triassic interface; therefore, this interface may supply a poor reflection coefficient. Multilobe reflections from the eastern Culpeper, Scottsville, and the Toano Seismic sections originate from rock units within the basin just above the floor of the basin. Reflections from within the basin cannot be resolved without the presence of an anomalously high/low velocity/density rock unit as was seen and modeled from the western Culpeper seismic section. Modeling of the western Culpeper seismic profile indicates that the lack of reflections seen below the basins in other seismic sections may be due to the complex structure of the basin above.

The Culpeper seismic lines indicate a basin with a maximum thickness of 2500-3000 m along the western side and 1400-1600 m along the eastern side. The basin fill along the western line consists of sediments and basalt flows that have been rotated as much as 40° along a listric normal

fault which may be related to an older structure below the basin. The eastern line in contrast contains relatively undisturbed, though gently dipping and faulted, strata along the bottom of the basin.

The Richmond data indicate a complex structure near the base and below the basin. The refraction data indicate this structure may be similar to a horst-graben type structure. The maximum thickness of the basin could not be determined from the seismic data; however, the shallow outlier to the west of the main basin is only 700-800 meters thick. This agrees with the thickness calculated by Mickus and others (1985) using gravity in this area; therefore, it is likely that their calculation of the thickness for the deepest part of the seismic line as 2700 m is accurate. ZOP analysis indicate numerous faults and gentle folds near the surface of the basin.

The Scottsville data did not image the basin clearly. This is attributed to the low velocity contrasts between the basin and the surrounding country rock. Termination and changes in the character of reflections on either side of the basin are used to interpret the geometry of that basin. The eastern side of the basin is shallower than the western side. A profile of the basin resembles the profile of a ladle. The eastern side of the basin reaches a thickness of 800-900 m and the central and western side of the basin reaches a thickness of 1750 m. As with the Richmond data, the contents and the geometry of the contents of the Scottsville Basin could not be determined.

Seismic data from the Toano basin indicate the presence of a basin which appears to much more symmetrical than the other basins. This basin may be as thick as the Culpeper Basin reaching a possible thickness of 3000 m. The fact that lignite was recovered from a well north of this seismic line (Brown and others, 1972) has been used to infer that reflections seen on the seismic section here are due to lignite or perhaps coal beds.

Conclusions

The investigations of the seismic reflection data obtained from the Triassic-Jurassic basins in Virginia indicate low impedence contrasts between the rock units within the basin and those bordering it is the primary reason for the lack of reflections from these interfaces. Complex geometry accompanied with low impedance contrasts does not allow the full benefits of multi-fold data acquisition and processing to be achieved. Large amplitude reflections from within the basin in these profiles can be attributed to anomalously high/low velocity/density rocks within the basin such as basalt or lignite. Geometries of the basins are determined from abruptly terminated reflections and indicate that the thickness of these basins range from 1750-3000 m. CORP analysis of the refracted arrivals in the seismic data can resolve apparent velocities for the refracting interface in particular if data is recorded with a split-spread receiver geometry. ZOP and CZOP analysis can aid in interpreting the geometry of the near surface geology and offers a way to extract more information from seismic reflection data with long receiver spread configurations. Velocities of the material within these basins, as determined from CORP analysis have a range of 4000-5300 m/sec.

BIBLIOGRAPHY

Bally, A. W., 1981, Atlantic type margins, in Bally, A. W., eds., Geology of passive continental margins: history, structure, and sedimentological record (with special emphisis on the Atlantic margin): American Association of Petroleum Geologists, education Course Note Series No. 19, p. 1-1 - 1-48.

Barry, K. M., 1967, Delay time profile interpretation, in Musgrave, A. W., ed., Seismic refraction prospecting: Society of Exploration Geophysicists, p. 348-357.

Bobyarchick, A. R., 1976, Tectogenesis of the Hylas Zone and eastern Peidmont near Richmond, Virginia [M.S. Thesis]:Blacksburg, Virginia Virginia Polytechnic Institute and State University, 168 p.

Bobyarchick, A. R., and Glover, L. III, 1979, Deformation and metamorphism in the Hylas Zone and adjacent parts of the eastern Peidmont in Virginia: Geological Society of America Bulletin Part I, v. 90, p. 739-752.

Bonner, B. P., and Schock, R. N., 1981, Seismic wave velocity, in Touloukian, Y. S., and Ho, C. Y., eds., Physical properties of rocks and minerals: McGraw Hill/Cindas data series on material properties, p. 221-256.

Brennen, J., 1985, Interpretations of Vibroseis reflections from within the Catoctin Formation of central Virginia [M.S. Thesis]; Virginia Polytechnic Institute and State University, Blacksburg, VA, 95 p.

Brown, P. M., Miller, J. A., and Swain, F. M., 1972, Structural and stratigraphic framework, and spatial distribution of permiability of the Atlantic Coastal Plain, North Carolina to New York: U. S. Geological Survey Professional Paper 796, 79 p.

Cordier, J., 1985, Velocities in reflection seismology: D. Reidel Publishing Co., Netherlands, 201 p.

Cornet, B., 1977, The palynostratigraphy and age of the Newark Basin [Ph.D. Thesis]; Pennsylvania State University, 506 p.

Çoruh, C., and Costain, J. K., 1983, Noise attenuation by Vibroseis whitening VSW processing, Geophysics, v 48, p. 543-554.

D'Angelo, R., 1985, Correlation of seismic reflection data with seismicity over the Ramapo, New Jersey, fault zone [M.S. Thesis]: Blacksburg, Virginia Polytechnic Institute and State University, 82 p.

Drake, A. A. Jr., and Morgan, B. A., 1981, The Piney Branch Complex - A metamorphosed fragment of the central Appalachian ophiolite in northern Virginia, American Journal of Science, v. 281, no. 3, p. 484 - 508.

Drake, A. A. Jr., 1986, Geologic map of the Fairfax County quadrangle, Fairfax County, Virginia: U. S. Geological Survey Geologic Quadrangle Map GQ-1600, scale 1:24,000.

Espenshade, G. H., and Clarke, J. W., 1976, Geology of the Blue Ridge Anticlinorium in northern Virginia: Geological Society of America Field Trip Guidebook No. 5, 26 p.

Faill, R. T., 1973, Tectonic development of the Triassic Newark-Gettysburg Basin in Pennsylvania, Geological Society of America Bulletin, v. 84, p. 725 - 740.

Farrar, S. S., 1984, The Goochland granulite Terrane: remobilized Grenville basement in eastern Virginia Piedmont; in Bartholomew, M. J. ed., The Grenville Event and the Appalachians and related topics, Geological Society of America Special Paper 194, p. 215-227.

Glover, L. III, Poland, F. B., Tucker, R. D., and Bourland, W. C., 1980, Diachronous Paleozoic mylonites and structural heredity of Triassic-Jurassic Basins in Virginia: Geological Society of America Abstracts with Programs, v. 8, p. 178.

Goodwin, B. K., 1970, Geology of the Hylas and Midlothian quadrangles, Virginia: Virginia Division of Mineral Resources Report of Investigations 23, 51 p.

Johnson, S. S., 1973, Bouguer Gravity Northeastern Virginia and the eastern shore Pennsylvania: Virginia Division of MIneral Resources Report of Investigations 32, 48 p.

Johnson, S. S., 1975, Bouguer gravity in Southeastern Virginia: Virginia Division of Mineral Resources, Publication 39, 42 p.

Johnson, S. S., and Froelich, A. J., 1982, Aeromagnetic contour map of the Culpeper Basin and vicinity, Virginia: Virginia Division of Mineral Resources Publication 41, scale 1:125,000.

Leavy, B. D., Froelich, A. J., and Abram, E. C., 1983, Bedrock map and geotechnical properties of rocks of the Culpeper Basin and vicinity, Virginia and Maryland: U. S. Geological Survey, Miscellaneous Investigations series Map I-1313-C, scale 1:125,000.

Lee, K. Y., 1979, Triassic-Jurassic geology of the northern part of the Culpeper Basin, Virginia and Maryland: U. S. Geological Survey, Open-file Report 79-1557, 17 pages.

Lee, K. Y., 1980,Triassic-Jurassic Geology of the southern part of the Culpeper Basin, Virginia: U. S. Geological Survey Open-file Report 80-468, 16 pages.

Lindholm, R. C., 1978, Triassic-Jurassic faulting in eastern North America - a model based on pre-Triassic structures: Geology, v. 6, p. 365-368.

Lindholm, R. C., 1979, Geologic history and stratigraphy of Triassic - Jurassic Culpeper Basin, Virginia: Summary: Geological Society of America Bulletin Part I, v. 90, p. 995-997.

Manspeizer, W., 1981, Early Mesozoic basins of the central Atlantic passive margins, in Bally, A. W., ed., Geology of passive continental margins: history, structure, and sedimentologic record (with special emphasis on the Atlantic margin): American Association of Petroleum Geologists Education Course Note Series No. 19, p. 4-1 - 4-60.

March, D. W., and Bailey, A. D. ,1982, A review of the two-dimensional transform and its use in seismic processing: Technical Paper presented at 44th meeting of the European Association of Exploration Geophysicists, 45 pages.

Mickus, K. C., Aiken, L. V., and Ziegler, D.,1985, Integrated geophysical study of the Triassic Richmond Basin, Virginia: Society of Exploration Geophysicists Expanded Abstracts of the Technical Program, p. 210-212.

Nelson, W. A., 1962, Geology and mineral resources of Albemarle County, Virginia Division of Mineral Resources Bulletin 77, 92 pages.

Petersen, T. A., Brown, L. D., Cook, F. A., Kaufman, S., and Oliver, J. E., 1984, Structure of the Riddleville Basin from COCORP seismic data and implications for reactivation tectonics: Journal of Geology, v. 92, p. 261-271.

Poland, F. B., 1976, Geology of the rocks along the James River between Sabot and Ceder Point, Virginia [M.S. Thesis]:Blacksburg, Virginia Polytechnic Institute and State University, 98 p.

Ratcliffe, N. M., 1971, The Ramapo fault system in New York and adjacent New Jersey: A Case of tectonic heredity, Geological Society of America Bulletin, v. 82, p. 125-142.

Ratcliffe, N. M., Burton, W. C., D'Angelo, R. M., and Costain, J. K., 1986, Seismic reflection geometry of the Newark Basin margin in eastern Pennsylvania, evidence for extensional reactivation of Paleozoic thrust faults: U. S. Nuclear Regulatory Commission Technical Report NUREG/CR-4676, 21 p.

Roberts, J. K., 1928, The Virginia Triassic: Virginia Geological Survey Bulletin 29, 205 p.

Robinson, E. A., and Treitel, S., 1980, Geophysical Signal Analysis: New Jersey, Prentice Hall, Inc., 466 p.

Reilly, J. M., 1980, A geologic and potential field investigation of the central Virginia Peidmont [M.S. Thesis]: Blacksburg, Virginia Polytechnic Institute and State University, 111 p.

Sengbush, R. L., Lawrence, P. L., and McDonal, F. J., 1061, Interpretation of synthetic seismigrams; Geophysics, v. 26, p. 138-157.

Taner, M. T., and Koehler, F., 1969, Velocity spectra - digital computer derivation and applications of velocity functions: Geophysics, v. 34, p. 859-881.

Zietz, I., Calver, J. L., Johnson, S. S., and Kirby, J. R., 1977, Aeromagnetic map of Virginia: in color: Virginia Division of Mineral Resources Geophysical Investigations Map GP 916, scale 1:1,000,000.

Appendix A. Data Acquisition and Processing

Data Acquisition

Seismic reflection lines over the Culpeper, Richmond, and Scottsville Basins were all obtained from a single Failing Y-1100 compressional wave vibrator from the Regional Geophysical Laboratory, Department of Geological Sciences at Virginia Polytechnic Institute and State University. The seismic line located along Interstate 64 over the Coastal Plain was obtained by Geophysical Services Incorporated. Table 1 on page 61 lists recording parameters for the various reflection lines.

The data acquisition parameters used in the Culpeper and the Scottsville surveys were designed to image the shallow basins. The seismic line over the western Culpeper basin resulted in a clear image of the basin and its composition, whereas the other seismic lines were only marginally successful in imaging the composition of the basins. The complex geology, poor reflectivity of the sediments, and shallowness of the bottom of the basins is assumed to be the primary cause for this lack of data within the western Culpeper and the Scottsville basins. Recording parameters for the Richmond seismic line were not conducive for the recovery of reflections from within that basin, which was recorded using a relatively far near-offset of 210

Table 1. Sweep and recording parameters

LINE NAME	START FREQUENCY	END FREQUENCY	SAMPLE RATE	DISTANCE BETWEEN VIBRATOR POINTS	RECEIVER GROUP INTERVAL	NEAR OFFSET & (FOLD)
Culpeper East Shots 1-90	80 Hz	10 Hz	2 ms	35 m	35 m	70 m (24)
Culpeper East Shots 91-206	58 Hz	10 Hz	2 ms	35 m	35 m	105 m (24)
Culpeper West	58 Hz	10 Hz	2 ms	35 m	35 m	105 m (24)
Richmond	60 Hz	10 Hz	2 ms	140 m	70 m	350 m (12)
Scottsville	80 Hz	10 Hz	2 ms	35 m	35 m	70 m (24)
Toano	14 Hz	56 Hz	4 ms	134 m	67 m	201 m (24)

m and 12-fold geometry. The mute pattern cut the already low fold down to virtually nothing for the shallow (0.0 - 0.5 sec) data.

Data Processing

All the data were processed on a VAX 11/780 located at the Regional Geophysical Laboratory using Digicon Incorporated's DISCO seismic software. The general processing sequence consisted of defining the geometry, recorrelation of the data, hand-editing and picking velocities for derivation of datum statics, sorting and application of datum statics, and then a complex interaction between picking velocities, mutes, and surface consistent residual statics. Once a final stacked section was derived through this process, various bandpass filters were tested, and finally a finite difference migration performed. This resulted in an interpretable section. Detailed velocity analyses were carried out during the interpretation of the data to define a general velocity function for the Triassic of Virginia.

Special processing problems were encountered in some of the data. The western Culpeper, Scottsville, and Interstate 64 data all required predictive deconvolution for the removal of reverberations. The western Culpeper line required an F-K filter for the removal of a surface wave on the shot records.

Geometry

The geometry was defined for the various surveys to correct for skipped shots and other problems in the field. The CDP line was defined at this point so that the subsurface coverage was perpendicular to the surface geology, while maintaining a consistently high-fold coverage.

Correlation

The data from the Culpeper, Richmond and I-64 basins were recorrelated beyond the sweep length to increase the time of the section, yielding more data with less field work. For

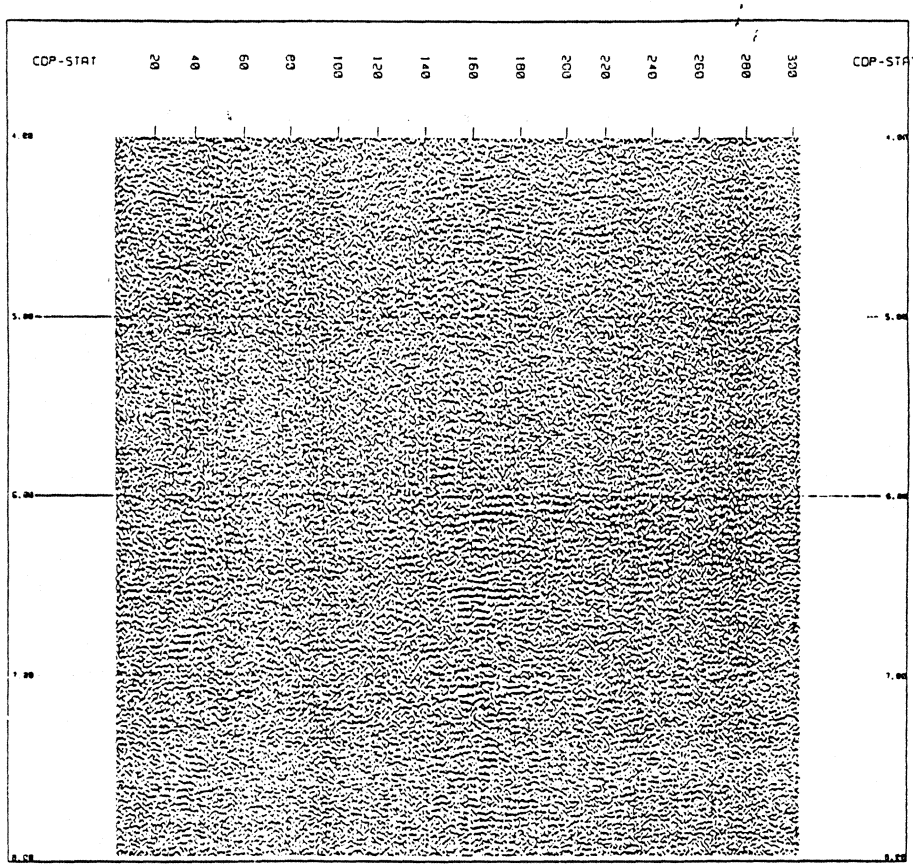

Figure 30. Western Culpeper: After correlation beyond the sweep length.

Table 2. Recorrelation parameters

LINE NAME	FREQUENCY SWEEP	SWEEP LENGTH	RECORD LENGTH	OLD LENGTH OF DATA	NEW LENGTH OF DATA	IDEAL FREQUENCY SWEEP AT END OF NEW DATA
Culpeper East Shots 1-90	80-10 Hz	17 s	21 s	4 s	11 s	80-39 Hz
Culpeper East Shots 91-206	58-10 Hz	17 s	21 s	4 s	11 s	58-29 Hz
Culpeper West	58-10 Hz	18 s	21 s	3 s	11 s	58-31 Hz
Richmond	60-10 Hz	22 s	29 s	7 s	9 s	60-15 Hz
Toano	14-56 Hz	10 s	18 s	8 s	14 s	14-31 Hz

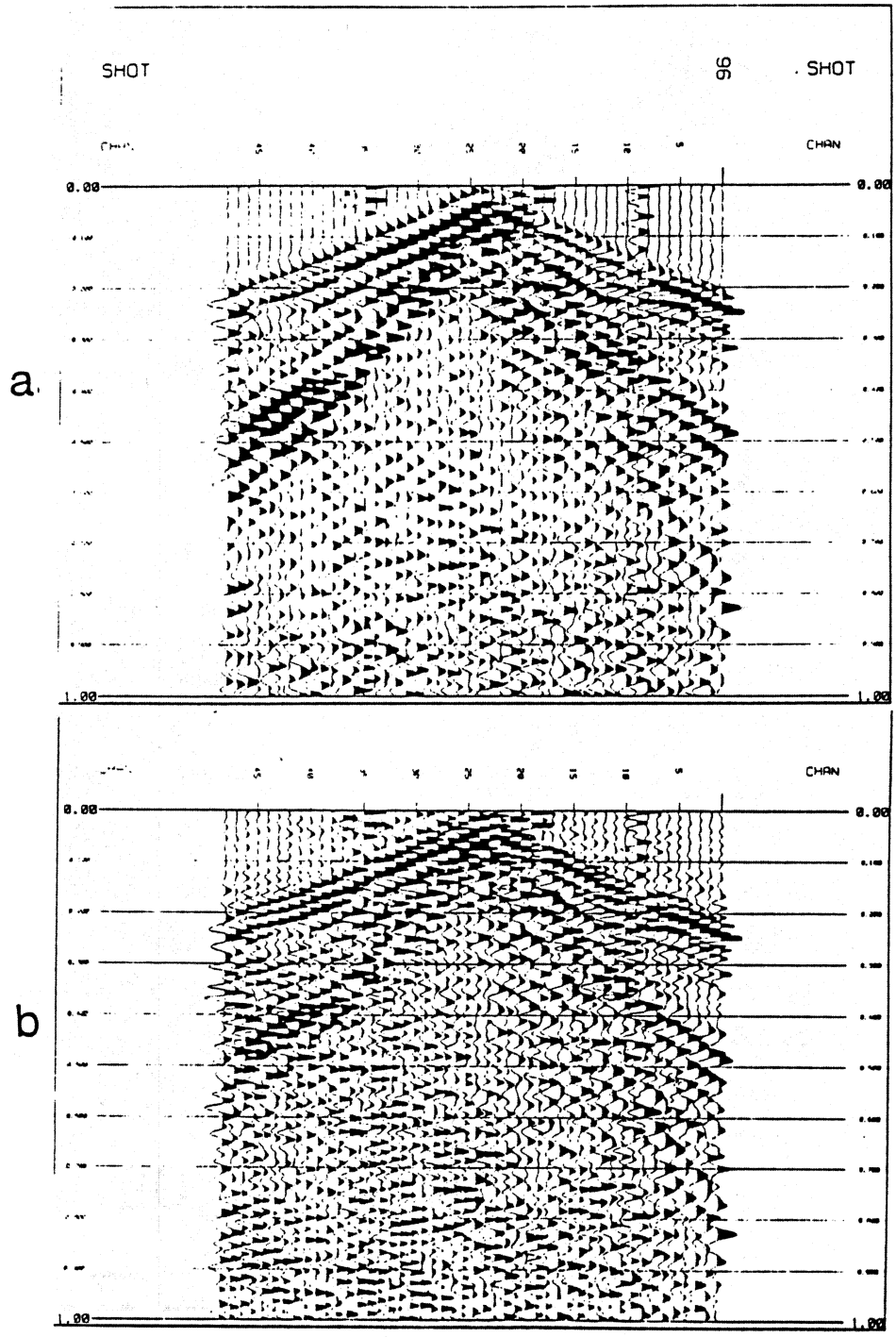

Figure 31. Vibroseis whitening: Comparison of CDP data from Eastern Culpeper line before (a) and after (b) Vibroseis Whitening using 1000 ms window.

example, the western Culpeper line initially had a sweep length of 18 sec and a record length of 21 sec, which would provide four sec of data with a full frequency content of 58-10 Hz. By padding the length of the record with 8 sec of zeros and then correlating the data as if the record length were actually 29 sec, the data is increased in length from 3-11 sec. The sweep trace of the western Culpeper line has a time rate of change of frequency content of 2.6 Hz per sec. Correlating beyond the sweep length results in a loss of frequencies in the data at the same rate beginning with the lower frequencies, due to the fact that the data was acquired with a sweep from high to low frequencies. At the very end of the data (11 sec) the ideal frequency content consists of 58-31 Hz. Even with this loss of frequencies, reflections were recovered from as deep as seven sec, as seen in Figure 30. Unfortunately, the deeper reflections did not appreciably help in the interpretation of the history of the basin formation. This extra data does, however, show that reflections exist as deep as 7.0-9.0 sec, which indicates that this area is not acoustically transparent (Figure 30). A list of the ideal frequency content before and after correlation beyond the sweep length can be found in Table 2 on page 64.

All the seismic lines had Vibroseis whitening (Çoruh and Costain 1983) applied prior to the correlation process. The resolution of the data has been found to be improved dramatically after Vibroseis whitening is applied. The data in Figure 31 shows data from the eastern Culpeper seismic line before and after Vibroseis whitening was applied.

Edit and Datum Statics

All the seismic lines were hand edited, and at the same time velocities were derived from the first breaks for use in determining the datum static shift to be applied. The majority of the traces thrown out were from the area of the roll-on and the roll-off. This raises the question as to whether the increase in subsurface coverage gained by the roll-on and roll-off outweighs the fact that most of the lost traces are in that region. Note that in general only one trace per shot was lost during the roll-on and roll-off; therefore, intuitively, it seems economical to gain the extra CDP coverage.

Table 3. Datum calculations

LINE NAME	MINIMUM ELEVATION (METERS)	MAXIMUM ELEVATION (METERS)	DATUM ELEVATION (METERS)	DATUM VELOCITY (METERS PER SECOND)
Culpeper East	49	72	65	4300
Culpeper West	100	255	200	4600
Richmond	41	116	100	4500
Scottsville	123	169	160	5000
Toano	7	35	25	2000

Datum statics were derived and applied based on velocities gleaned from the first breaks on the shot records. The datum velocities and elevations along with the minimum and the maximum elevation are listed in the recording parameters (Table 3 on page 67).

Deconvolution

The western Culpeper, Scottsville, and Toano data contained reverberations. To remove these reverberations, and therefore whiten the frequency spectrum, all the data were deconvolved using predictive deconvolution (Robinson and Trietel, 1980). Autocorrelations of the data from the western Culpeper line before and after deconvolution are shown in Figure 32. The common depth point gathers of the western Culpeper basin data before and after deconvolution are shown in Figure 33. Note the increased resolution in the CDP gathers at 0.7 and 1.0 sec along with the fuller frequency content throughout. A stacked section of the western Culpeper line before and after predictive deconvolution is illustrated in Figure 34. The deconvolved section exhibits an improvement in the sharpness and number of reflections which were previously obscured by the reverberations. The Toano Basin (Figure 35) and the Scottsville basin also benefitted from predictive deconvolution. The gap and filter length used on the data are listed in Table 4.

Two Dimensional Filtering

The eastern Culpeper data suffered from a severe noise problem in the form of surface waves. This noise was especially acute in that the basin does not extend below 0.7 sec on this section and the surface waves extend to depths of 0.4-1.0 sec. This inhibited the recovery of reflections from within the basin.

An F-K filter was designed, using an unconventional method, for the removal of the surface waves. The data were split-spread and therefore contained both negative and positive offsets. The conventional filter design would either remove or leave a specified wedge within the F-K domain. Filtering the data in shot-ordered sort would require removal of a significant portion of the F-K space, thereby decreasing the effectiveness of the filter (March and Bailey, 1982).

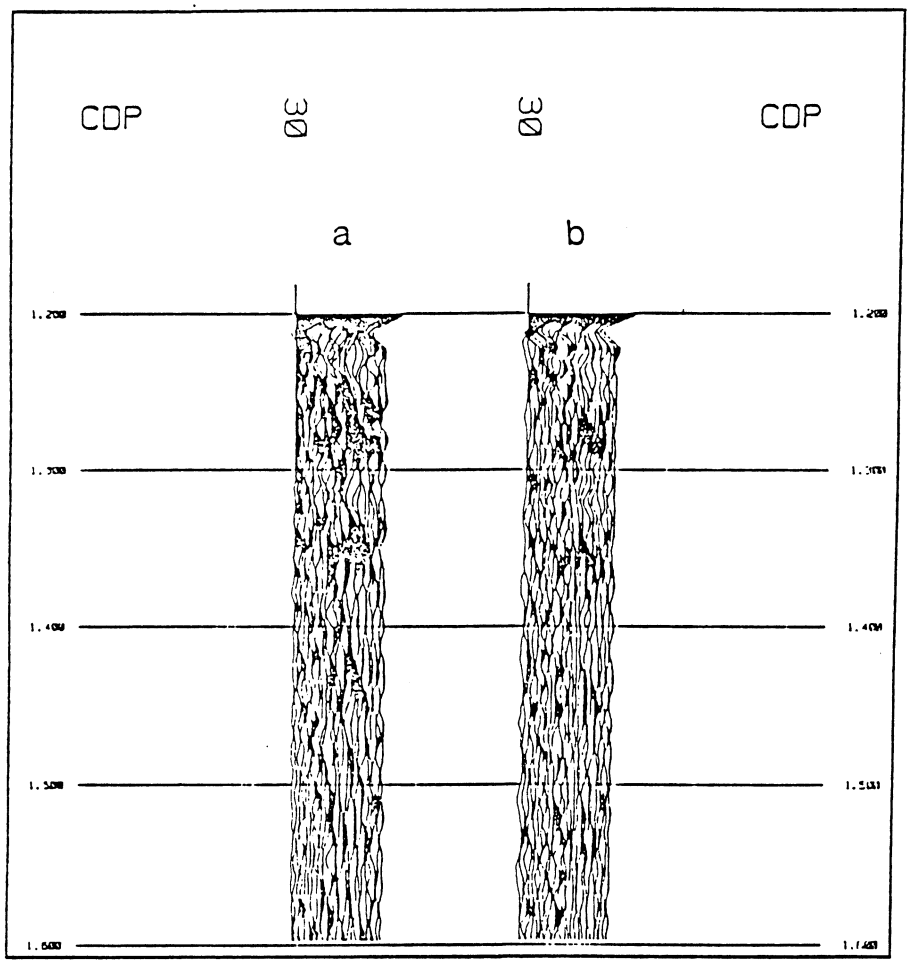

Figure 32. Autocorrelations: Western Culpeper line a) before and b) after deconvolution.

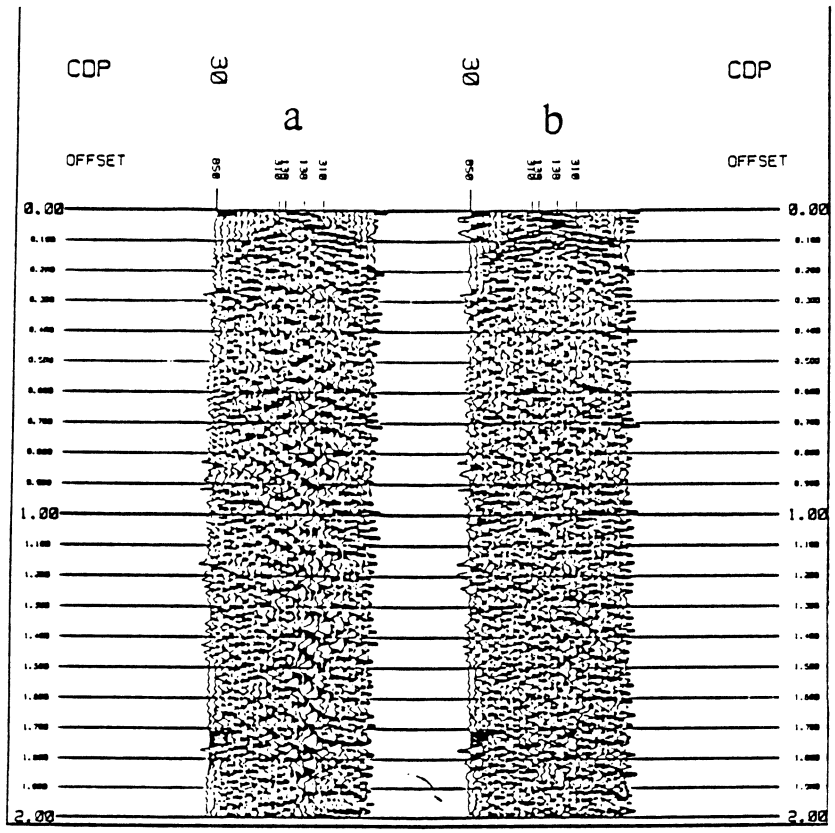

Figure 33. **Effects of deconvolution:** CDP gathers a) before and b) after deconvolution in the northern Culpeper seismic line.

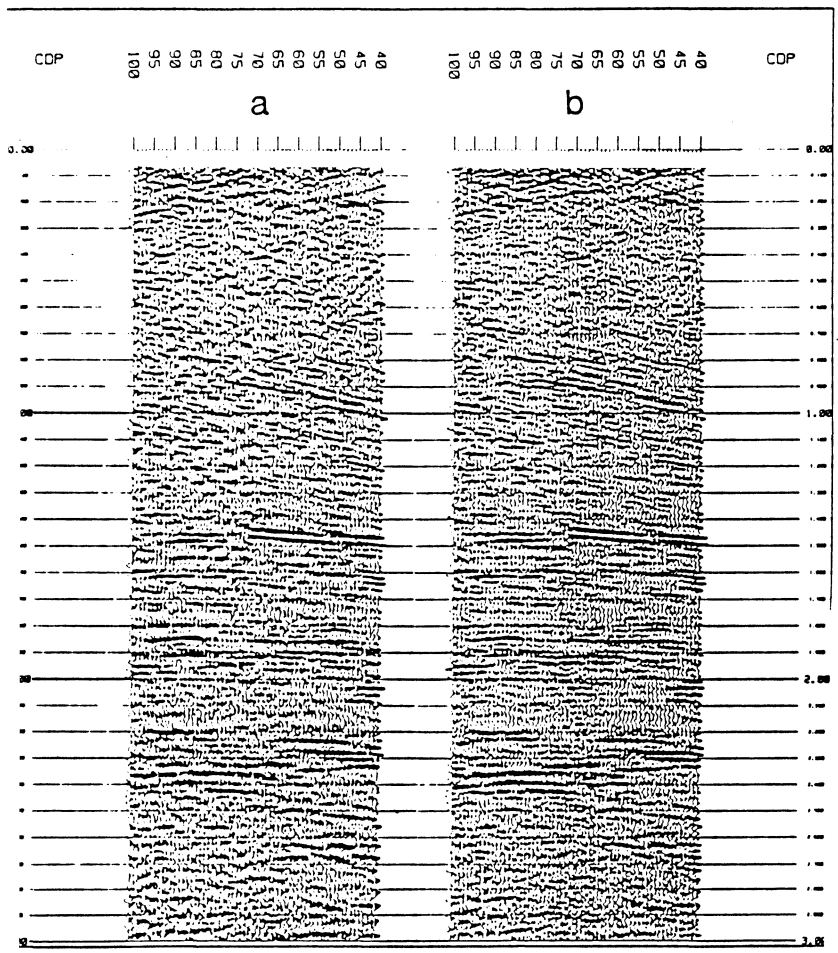

Figure 34. Effects of deconvolution: Stacked section of the western Culpeper seismic line a) before and b) after deconvolution.

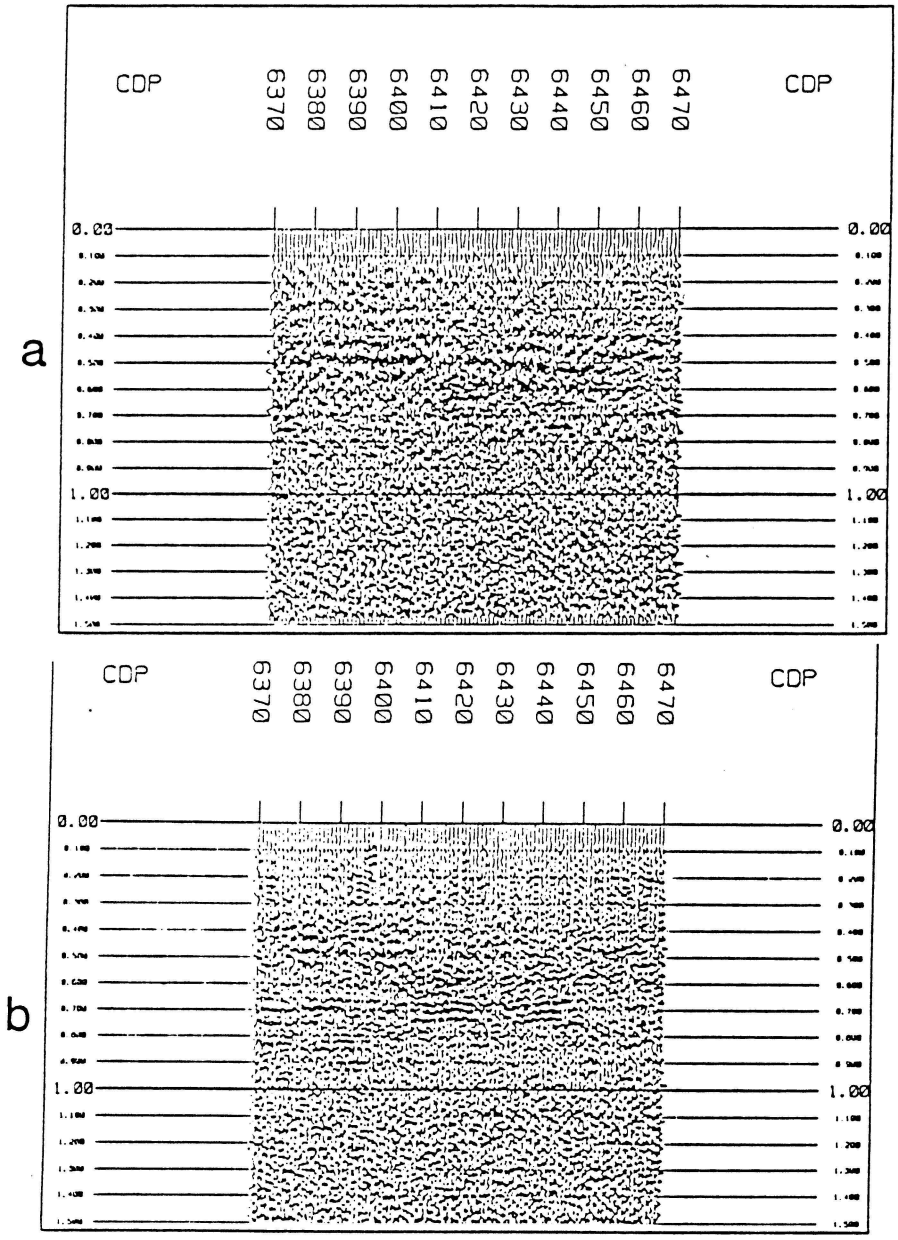

Figure 35. Effects of deconvolution: Stacked sections of the Toano Basin a) before and b) after deconvolution.

Table 4. Deconvolution parameters

LINE NAME	GAP LENGTH	FILTER LENGTH
Culpeper West	20 ms	80 ms
Scottsville	20 ms	70 ms
Toano	30 ms	104 ms

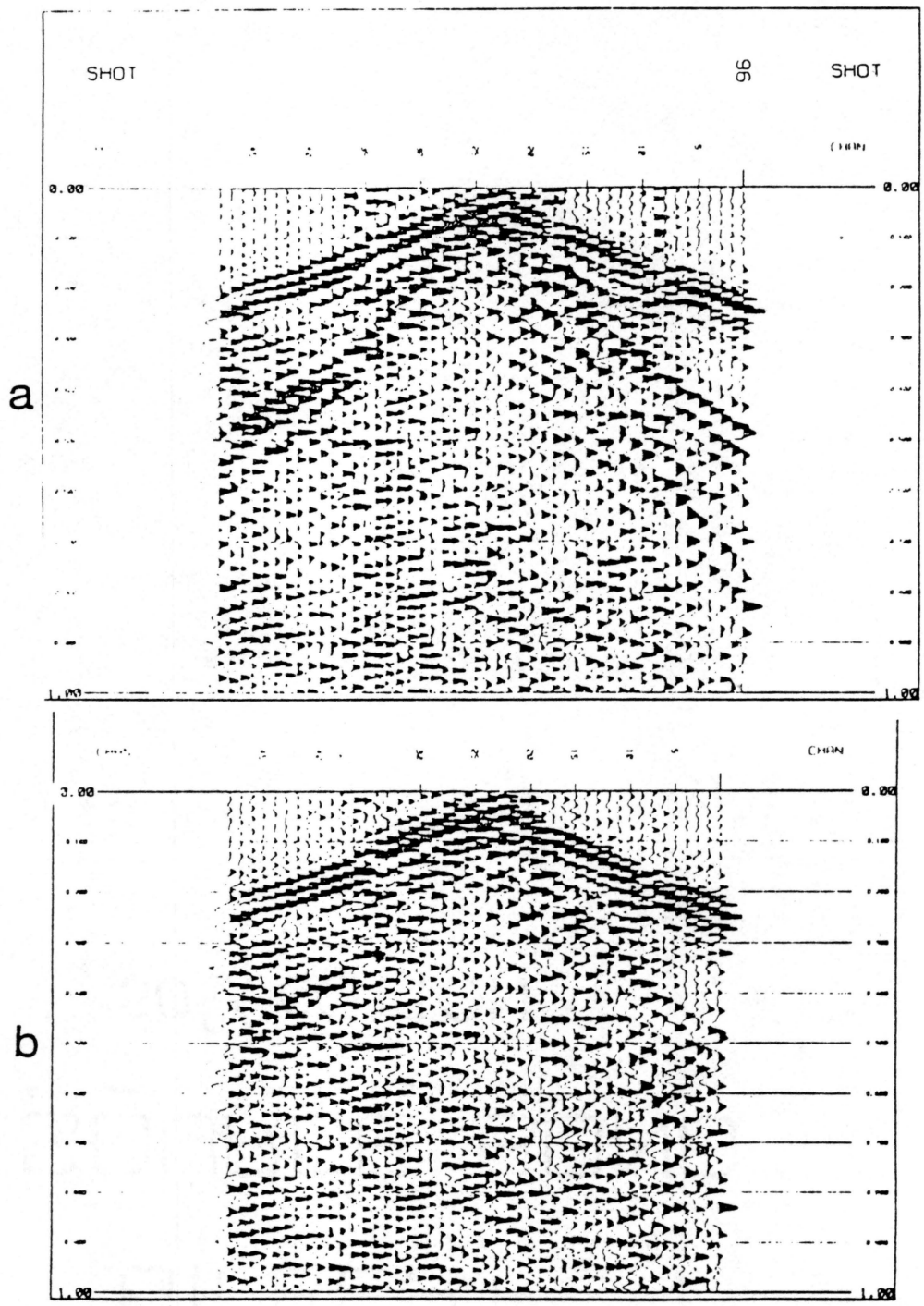

Figure 36. Surface waves: Shot records from the eastern Culpeper line a) before and b) after F-K filtering.

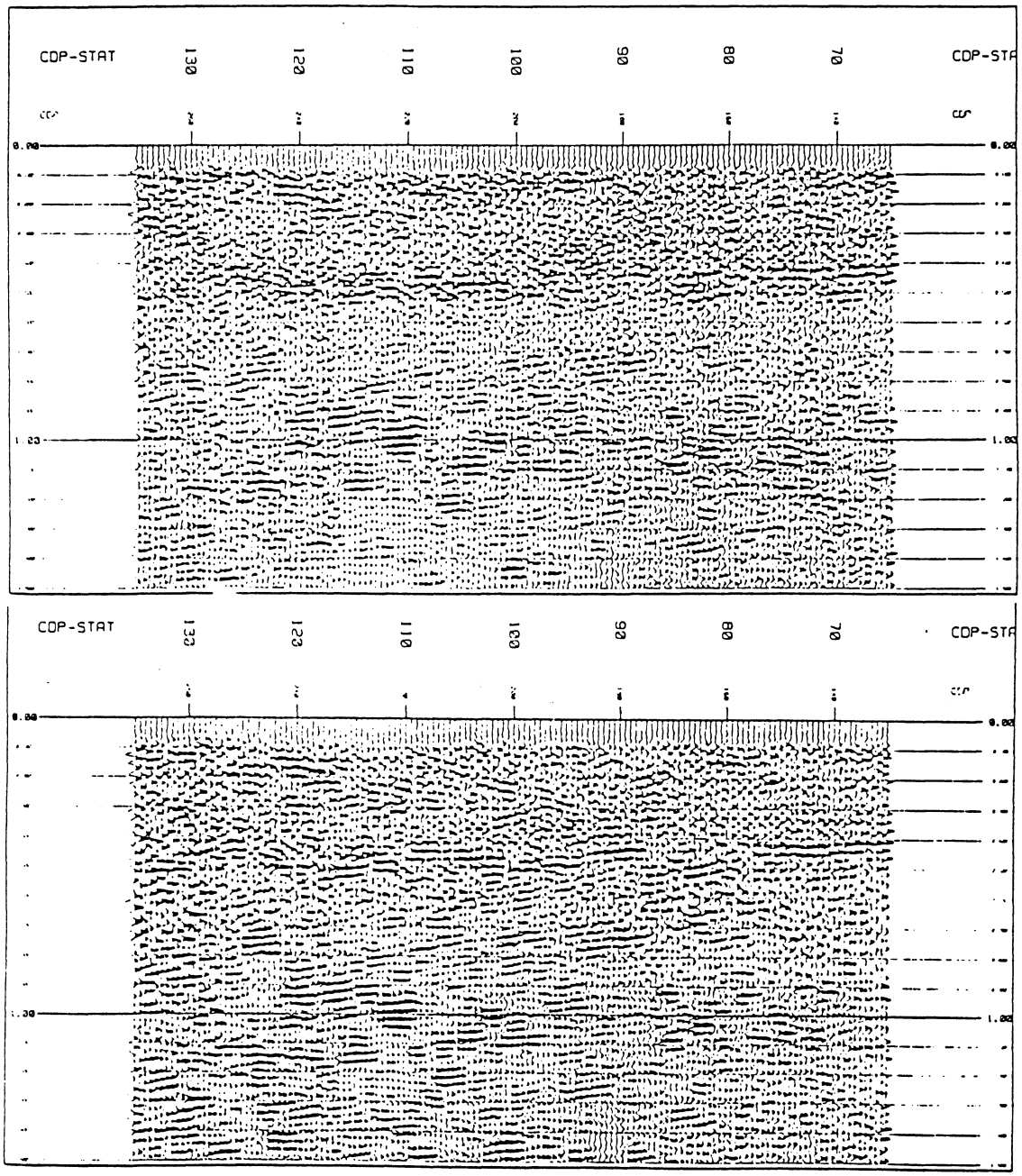

Figure 37. F-K filtering: Effects of two dimensional filter on the stacked section of the eastern Culpeper seismic line before (a) and after (b) F-K filtering.

Extensive testing revealed that the effectiveness of the filter was also dependent upon the coherence of the wave being filtered. The surface wave on either side of the zero offset point had different characteristics, as would be expected. Generally the shot records were sorted by signed offset. Trying to resort the shots by absolute value of the offset, thereby allowing a smaller window of the F-K domain to be filtered, resulted in better filtering; however, the coherency of the surface wave was degraded. The final filtering process began by splitting each shot into two separate records, one containing the negative offsets and one containing the positive offsets. Filters were then designed and applied upon each of these new data records. Thus, the window to be filtered in the F-K domain was reduced even further and the coherency of the surface wave was retained. The effects of the filtering on the shot records can be seen in Figure 36. The real test of the effectiveness of the filter can be seen on the stacked section (Figure 37).

Main Processing

The remainder of the processing involved iterations of picking velocities, mutes, and deriving surface consistent residual statics. After a final stacked section was derived, band pass filters were tested and a finite difference migration performed on the data. These steps resulted in the most significant increase in signal-to-noise ratio in the data; of the four steps, the residual statics best increased the data quality the best.

The general procedure involved deriving a brute stack while sorting the data into CDP gathers. After choosing a a general velocity function based upon velocities common to the area, a simple mute pattern was designed to eliminate primarily the first breaks. This brute stack was then used to choose time and spatial windows within which velocity analysis and residual statics determinations would be done. Velocity was analyzed using constant velocity panels and velocity spectra (Tanner and Kholer, 1969), while a mute pattern was designed as the velocities and residual statics were refined. This interaction was repeated until a best-stacked section was derived.

The most effective processing tool on all the data was the derivation and application of surface consistent residual statics. The statics problem may have been extremely acute over the basins due to the sedimentary strata overlying the metamorphic and igneous rock units, such as the Catoctin and the Petersburg Granite. The velocities were difficult, if not impossible, to determine without a proper residual static correction. Once the correct residual statics were applied to the data, then accurate velocities could be determined with much more confidence. The velocities were not as important as might be expected because the data over the Culpeper, Scottsville, and the I-64 Basins were recorded using short far offsets. Over such short offsets the maximum normal moveout may be no more than 20 ms and the minimum no more than 4 ms. The velocities would have played a much more important role in the Richmond basin data, due to the fact that the maximum offset there was considerably greater than that of the other lines; but most of the further offsets had to be muted out thereby obscuring the basin. This, and the high velocities associated with the Triassic-Jurassic sedimentary strata, made determining a velocity function to define the basins impossible using velocity spectra.

The mute pattern was crucial in uncovering the reflections from the sediments within the basins, in particular the Culpeper basin where reflectivity is good. This is easily understood when one considers that the deepest portion of the basins did not exceed 1.0-1.5 sec, while the mute pattern reached depths of 0.3 sec on the data from the shorter offsets (Culpeper, Scottsville, and I-64 basins) and reached depths of 0.6-0.7 sec on the Richmond basin.

The vita has been removed from the scanned document